Comparison of Microscopic and Endoscopic Approaches to the Cerebellopontine Angle

Yusuke Takemura, M.D.,[1] Tooru Inoue, M.D., Ph.D.,[2] Takashi Morishita, M.D., Ph.D.,[1] Albert L. Rhoton, Jr., M.D.[1]

[1] Department of Neurosurgery, University of Florida College of Medicine, Gainesville, Florida, USA

[2] Department of Neurosurgery, University of Fukuoka Faculty of Medicine, Fukuoka, Japan

Corresponding Author:

Albert L. Rhoton, Jr., M.D.

Department of Neurosurgery

P.O. Box 100265

Gainesville, FL, USA 32610-0265

Phone: 352-273-9000

Fax: 352-392-8413

rhoton@neurosurgery.ufl.edu

http://dx.doi.org/10.1016/j.wneu.2013.07.013

Comparison of Microscopic and Endoscopic Approaches to the Cerebellopontine Angle

ABSTRACT

Objective: The purpose of this study was to examine the efficacy of the endoscope as an adjunct to the operating microscope in defining the surgical anatomy of the cerebellopontine angle (CPA).

Methods: The surgical anatomy of the CPA was examined in cadaveric CPAs through a retrosigmoid approach. The upper, middle, and lower neurovascular complexes and the individual segments of the cerebellar arteries in the CPA were examined with the surgical microscope and 0^o and 45^o rigid endoscopes.

Results: The microscope provided satisfactory views of the posterior surface of the neural and vascular structures in the central part of the CPA cistern. The endoscope provided superior views of the nerves' junction with the brain stem, their dural exit, and their vascular relationships. The endoscope also provided superior views of the individual segments of the cerebellar arteries.

Conclusion: The combination of endoscopic and microsurgical techniques aids in achieving optimal exposure in CPA surgery.

Key words: Cerebellar arteries, Cerebellopontine angle, Cranial nerves, Endoscopy, Microsurgery.

Running head: Cerebellopontine Angle

Text Abbreviations: AICA, anterior-inferior cerebellar artery; CN, cranial nerve; CPA, cerebellopontine angle; MVD, microvascular decompression; PICA, posterior-inferior cerebellar artery; SCA, superior cerebellar artery; TN, trigeminal neuralgia.

INTRODUCTION

The high magnification and enhanced illumination provided by the endoscope have led to its use for cerebellopontine angle (CPA) exploration (9,15,16,21,25,31,32). Reported advantages of the endoscopic approach compared to the microscopic approach are that it allows for a smaller craniotomy, less dissection, minimal retraction, and more highly magnified focal exposures (1-5,7-9,11,15-18,20,21,24-26,31,32,37,38). The endoscope also provides a more precise view of the relationship of neurovascular structures to tumors and the offending vessel in vascular compression syndromes than is provided by the microscope (1,3,4,8,9,11,15,16,18,20,21,24-26,32). An understanding of the rich neurovascular relationships in the CPA is basic to complication avoidance. In this study, the exposure of structures in the CPA with the microscope and the endoscope were compared.

MATERIAL AND METHODS

Eleven adult cadaveric CPAs were examined using the 3X to 40X surgical microscope and 0^{o} and 45^{o} angle, 18-cm Hopkins endoscopes (Karl Storz GmbH & Co.), connected to a xenon light source and a high-definition camera after injection of the vessels with colored silicone. The neurovascular relationships in the CPA were examined by the retrosigmoid approach from the tentorium and third nerve above to the hypoglossal nerve and foramen magnum below. To standardize the comparison between the two surgical instruments, the CPA was divided into three parts (superior, middle, and inferior) and the cerebellar arteries into their individual segments (12,23,27,28,33,34).

RESULTS

Anatomic Overview

There are a number of structures occurring in sets of three in the CPA that can be grouped into upper, middle, and lower neurovascular complexes. These include the cerebellar arteries: superior (SCA), anterior-inferior (AICA), and posterior-inferior (PICA), parts of the brain stem (midbrain, pons, and medulla), cerebellar peduncles (superior, middle, and inferior), fissures between the brain stem and the cerebellum (cerebellomesencephalic, cerebellopontine, and cerebellomedullary), and the surfaces of the cerebellum (tentorial, petrosal, and suboccipital). When examining these relationships, three neurovascular complexes are defined: an upper complex related to the SCA, a middle complex related to the AICA, and a lower complex related to the PICA. Each neurovascular complex includes one of the three parts of the brain stem, one of the three surfaces of the cerebellum, one of the three cerebellar peduncles, and one of the three major fissures between the cerebellum and the brain stem. In addition, each neurovascular complex contains a group of CNs. The upper complex includes the oculomotor, trochlear, and trigeminal nerves that are related to the SCA. The middle complex includes the abducent, facial, and vestibulocochlear nerves that are related to the AICA. The lower complex includes the glossopharyngeal, vagus, accessory, and hypoglossal nerves that are related to the PICA.

Upper Complex

The upper complex includes the SCA, midbrain, cerebellomesencephalic fissure, superior cerebellar peduncle, tentorial surface of the cerebellum, and the oculomotor, trochlear, and trigeminal nerves. The SCA arises in front of the midbrain and passes below the oculomotor and trochlear nerves and above the trigeminal nerve to reach the cerebellomesencephalic fissure, where it runs on the superior peduncle and terminates by supplying the tentorial surface of the cerebellum.

The most common operation directed to the upper neurovascular complex is the exposure of the posterior root of the trigeminal nerve in trigeminal neuralgia. The posterior trigeminal root joins the brain stem about halfway between the upper and lower borders of the pons. Frequently, the superolateral lip of the cerebellomesencephalic fissure projects forward and obscures the junction of the posterior root with the pons. In its intradural course, the trigeminal nerve uniformly runs obliquely upward from the lateral part of the midpons to reach the upper surface of the petrous apex. It exits the posterior fossa to enter the middle cranial fossa by passing forward through the dural trigeminal porus located below the tentorial attachment to enter Meckel's cave.

At the junction of the trigeminal nerve with the pons, as many as 15 separate nerve rootlets may be spread around the rostral half of the site where the main sensory cone enters the pons (34). These rootlets are either aberrant sensory or motor rootlets. The aberrant sensory fibers are small rootlets that exit the pons outside the main sensory root around the rostral two-thirds of the nerve and usually join the main sensory root a short distance from the brain stem. There may be as many as eight aberrant roots (34). Motor rootlets also arise around the rostral part of the nerve; however, they tend to arise further from the main sensory root than do the accessory sensory rootlets. The motor root may be composed of 4 to14 separate rootlets, each having a separate exit from the pons (34).

The SCA arises in front of the midbrain and passes below the oculomotor nerve (33). It dips caudally and encircles the brain stem near the pontomesencephalic junction, passing below the trochlear nerve and above the trigeminal nerve. After passing above the trigeminal nerve, the SCA enters the fissure between the midbrain and cerebellum. On leaving the cerebellomesencephalic fissure where its branches are medial to the tentorial edge, its branches

pass posteriorly under the tentorial edge and are distributed to the surface facing the lower surface of the tentorium (tentorial surface). The SCA usually arises as a single trunk, but may also arise as a double (or duplicate) trunk. The SCAs arising as a single trunk bifurcate into a rostral and a caudal trunk. The rostral trunk supplies the vermian and paravermian part, and the caudal trunk supplies the hemisphere on the tentorial surface. The SCA frequently has points of contact with the oculomotor, trochlear, and trigeminal nerves.

SCA segments

The SCA is divided into 4 segments: (35)

Anterior Pontomesencephalic Segment, s1. This segment is located between the dorsum sellae and the upper brain stem. It begins at the origin of the SCA and passes below the oculomotor nerve to end at the anterolateral margin of the brain stem.

Lateral Pontomesencephalic Segment, s2. This segment begins at anterolateral margin of the brain stem and frequently dips caudally onto the lateral side of the upper pons. Its caudal loop projects toward, and may reach, the root entry zone of the trigeminal nerve at the midpontine level. This segment terminates at the anterior margin of the cerebellomesencephalic fissure. The trochlear nerve passes above the midportion of this segment.

Cerebellomesencephalic Segment, s3. This segment courses within the cerebellomesencephalic fissure. The SCA's branches enter the shallowest part of the fissure located above the trigeminal root entry zone and course medial to the tentorial edge with its branches intertwined with the trochlear nerve. This segment undergoes a number of hairpin turns within the fissure where its branches enter the superior cerebellar peduncles and supply the dentate nucleus.

Cortical Segment, s4. This segment includes the branches distal to the cerebellomesencephalic fissure that pass below the tentorium and are distributed to the tentorial surface of the cerebellum.

Contact occurs between the SCA and the trigeminal nerve in those cases with the most prominent caudally projecting loops. About half of the SCAs have a point of contact with the trigeminal nerve, which, depending on the site of bifurcation, may involve the main, rostral, caudal or both the rostral and caudal trunks, or a marginal hemispheric branch (33). Nearly two-thirds of SCAs have a point of contact with the oculomotor nerve, usually on the inferior surface (33). The segment of the trochlear nerve coursing along the lower margin of the tentorium was frequently intertwined with the SCA.

Microscopic View

The lateral infratentorial approach, directed between the tentorium and the lateral part of the tentorial surface of the cerebellum, was utilized for the examination of the upper part of the CPA because it requires less exposure of the other compartments and minimizes the exposure and risk to CNs VII and VIII (Fig. 1A). The first structures usually recognized in this approach are the superior petrosal veins draining into the superior petrosal sinus lateral to the nerve. These veins often blocked the view and access to the area around the trigeminal nerve (Fig. 1J). Significant venous retraction was often needed to see the trigeminal nerve and it was frequently necessary to divide a superior petrosal vein or one or more of its tributaries to gain access to the nerve. The most frequent finding in trigeminal neuralgia is that the SCA loops downward to compress the superomedial edge of the nerve (Fig. 1A). It was difficult to see the trigeminal nerve entering Meckel's cave due to prominences, especially the suprameatal tubercle, on the posterior surface of the temporal bone lateral to Meckel's cave (Fig. 1I and J). It was frequently

necessary to retract the anterior-superior lip of the cerebellum forming the lateral edge of the cerebellomesencephalic fissure to see the part of the trigeminal nerve adjacent the brain stem. The posterior surface of the trigeminal nerve and adjacent SCA were commonly seen. This approach provided satisfactory exposure of the posterior part of the s2 and the proximal cortical (s4) branches, which exit the lateral part of the cerebellomesencephalic fissure and run on the lateral part of the cerebellar surface facing the tentorium (Fig. 1A). It was difficult to see the s1, the part of the s2 looping downward medial to the trigeminal nerve, and the s3 coursing in the cerebellomesencephalic fissure. The segment of the trochlear nerve coursing between the lower surface of the tentorium and the SCA could be seen (Fig. 1A).

Endoscopic View

Advancing the 0^{o} endoscope deep to the craniotomy margin and under the tentorium provided good visualization of the superior petrosal veins, the posterior surface of the trigeminal nerve, the relationship of the s2 to the trigeminal nerve, and the cortical branches forming the s4 (Fig. 1B and L to N). Advancing the 0^{o} and 45^{o} endoscopes above the trigeminal nerve exposed the proximal part of the s1, the oculomotor and trochlear nerves, and the posterior cerebral and posterior communicating arteries in the lateral aspect of the interpeduncular cistern (Fig. 1O to Q). Directing the 45^{o} scope medially allowed viewing of the junction of the trigeminal nerve with the brain stem, which is often seen only when retracting the anterior-superior lip of the cerebellomesencephalic fissure in the microscopic view (Fig. 1C and D). It also provided a better view than the microscope of the relationship of the trigeminal sensory root to the motor and aberrant sensory rootlets at the junction with the pons (Fig. 1H). Directing the angled endoscope laterally provided a far better view of the porus of Meckel's cave than could be achieved with the microscope especially when there was a prominent suprameatal tubercle that blocked the

microscopic view of the trigeminal segment just proximal to Meckel's cave (Fig. 1E to H). Directing the endoscope downward from above the trigeminal nerve provided excellent views of the upper and anterior-superior surfaces of the nerve (Fig. 1E and G) and directing the endoscope upward from below the nerve provided excellent views of the lower and anterior-inferior surfaces of the nerve (Fig. 1F). Advancing the 45^{o} endoscope above CN V provided views of CN IV entering the tentorial edge, CN III passing below the uncus, and the arteries and membranes bordering the interpeduncular cistern (Fig. 1O to T).

Middle Complex

The middle complex includes the AICA, pons, middle cerebellar peduncle, cerebellopontine fissure, petrosal surface of the cerebellum, and the abducens, facial, and vestibulocochlear nerves. The AICA arises at the pontine level and courses in relationship to the abducens, facial, and vestibulocochlear nerves to reach the surface of the middle cerebellar peduncle, where it courses along the cerebellopontine fissure and terminates by supplying the petrosal surface of the cerebellum. The most common operations directed to the middle complex are for the removal of acoustic neuromas and other tumors, and for microvascular decompression for relief of hemifacial spasm. The examination of the middle level focused on relationships of the facial and vestibulocochlear nerves, internal acoustic meatus, and adjacent cerebellar arteries.

Meatal relationship

The nerves in the lateral part of the internal acoustic meatus are the facial, cochlear, and inferior and superior vestibular nerves. The position of the nerves is most constant in the lateral portion of the meatus, which is divided into superior and inferior portions by a horizontal ridge called either the transverse or falciform crest. The facial and the superior vestibular nerves are superior to the crest. The facial nerve is anterior to the superior vestibular nerve and is separated

from it at the lateral end of the meatus by a vertical ridge of bone called the vertical crest. The vertical crest is also called “Bill’s bar” in recognition of William House’s role in focusing on the importance of this crest in identifying the facial nerve at the fundus of the internal acoustic meatus. The cochlear and inferior vestibular nerves run below the transverse crest with the cochlear nerve located anteriorly.

Brain stem relationship

The landmarks on the brain stem side of the CPA that are helpful in guiding the surgeon to the junction of the facial and vestibulocochlear nerves with the brain stem are the pontomedullary sulcus; the junction of the glossopharyngeal, vagus, and spinal accessory nerves with the medulla; and the choroid plexus and flocculus protruding from the foramen of Luschka. The facial nerve arises from the brain stem near the lateral end of the pontomedullary sulcus 1 to 2 mm anterior to the point at which the vestibulocochlear nerve joins the brain stem at the lateral end of the pontomedullary sulcus, and 2 to 3 mm above the rostral end of a line directed along the origin of the rootlets of CNs IX, X, and XI from the medulla. The separation between the vestibulocochlear and facial nerves is greatest at the level of the junction of the nerves with the brain stem and decreases as these nerves approach the meatus. The filaments of the nervus intermedius are seen between the facial and vestibulocochlear nerves.

The structures related to the lateral recess of the fourth ventricle that have a consistent relationship to the facial and vestibulocochlear nerves are the foramen of Luschka, its choroid plexus, and the flocculus. The foramen of Luschka is situated at the lateral margin of the pontomedullary sulcus, just behind the junction of the glossopharyngeal nerve with the brain stem, and immediately inferior to the junction of the facial and vestibulocochlear nerves with the brain stem. A consistently identifiable tuft of choroid plexus, however, hangs out of the foramen

of Luschka and sits on the posterior surface of the glossopharyngeal and vagus nerves just inferior to the junction of the facial and vestibulocochlear nerves with the brain stem.

The AICA originates from the basilar artery, usually as a single trunk, and encircles the pons near the abducent, facial, and vestibulocochlear nerves. After coursing near and sending branches to the nerves entering the acoustic meatus and to the choroid plexus protruding from the foramen Luschka, it passes around the flocculus on the middle cerebellar peduncle to supply the lips of the cerebellopontine fissure and the petrosal cerebellar surface, which faces the posterior surface of the temporal bone. It commonly bifurcates near the facial-vestibulocochlear nerve complex to form a rostral and a caudal trunk. The rostral trunk courses above the flocculus and sends its branches laterally along the middle cerebellar peduncle to the superior lip of the cerebellopontine fissure and the adjoining part of the petrosal surface, and the caudal trunk courses below the flocculus to supply the inferior part of the petrosal surface.

AICA segments

The AICA is divided into 4 segments: (35)

Anterior Pontine Segment, a1. This segment, located between the clivus and the belly of the pons, begins at the origin and ends at the level of a line drawn through the long axis of the inferior olive. This segment usually lies in contact with the rootlets of the abducent nerve.

Lateral Pontine Segment, a2. This segment begins at the anterolateral margin of the pons and courses through the CPA by passing above, below, or between the facial and vestibulocochlear nerves. This segment is divided into premeatal, meatal, and postmeatal portions. This segment gives rise to the nerve-related branches that course near or within the internal acoustic meatus in close relationship to the facial and vestibulocochlear nerves. These nerve-related branches are the labyrinthine artery, which supplies the facial and

vestibulocochlear nerves and vestibulocochlear labyrinth; the recurrent perforating arteries, which pass toward the meatus but turn medially to supply the brain stem; and the subarcuate artery, which enters the subarcuate fossa on the posterior surface of the temporal bone lateral to the internal acoustic meatus.

Flocculopeduncular Segment, a3. This segment begins where the artery passes rostral or caudal to the flocculus to reach the middle cerebellar peduncle and ends where the branches cross the cerebellopontine fissure to reach the petrosal surface of the cerebellum.

Cortical Segment, a4. This segment is composed of the cortical branches to the petrosal surface.

Microscopic View

Our commonly selected approach to the middle neurovascular complex is directed along the lower and anterior margins of the flocculus and is referred to as an infrafloccular approach. This approach is directed medially along the posterior margin of the CN IX with rostral retraction of the choroid plexus and flocculus protruding from the foramen of Luschka in order to expose the posterior surface of CNs VIII and IX at the brain stem. Elevating the choroid plexus and flocculus rostrally avoids lateral to medial retraction, which may tear the filaments of the cochlear nerve at the lamina cribrosa in the fundus of the meatus with a resulting hearing loss (34). Elevating the flocculus allows viewing of the junction of CN VII with the brain stem in the area anterior-inferior to the brain stem junction of CN VIII (Fig. 2A). This approach with the microscope provides a view of the posterior surface of the facial and vestibulocochlear nerves and the meatal and postmeatal segments of the a2. The abducens nerve may occasionally be seen ascending anterior to the pons. In this approach, the segment of the facial nerve adjacent the brain stem is seen below the vestibulocochlear nerve, but the facial nerve ascends to be hidden

anterior to CN VIII as it approaches the meatal porus where it can be seen with gentle elevation or depression of CN VIII (Fig. 2A). After removing the posterior wall of the internal acoustic meatus, the individual nerves in the proximal and mid meatus may be seen, the transverse and horizontal crests at the meatal fundus may be palpated with a fine dissector, but are often difficult to see (Fig. 3A, B, and E). The a2 at the level of CNs VII and VIII and the a3 and a4 are frequently exposed, but the a1 in front of the brain stem is not seen. Other branches of the a2 that may be seen are the labyrinthine arteries joining CNs VII and VIII, the subarcuate artery entering the dura, and the recurrent perforating arteries returning to the brain stem between CNs VII and VIII (Fig. 2A).

Endoscopic View

The 0^{o} endoscope positioned with the tip just deep to the dura, after elevating the flocculus and choroid plexus, provides a view of CN VIII from brain stem to porus and the segment of CN VII near the brain stem, but the segment of CN VII adjacent the meatal porus is seen only with gentle retraction of CN VIII (Fig. 2B). The AICA segments at the level of, and posterior to, the nerves and their labyrinthine and subarcuate and recurrent perforating branches are seen (Fig. 2B and I). Advancing the straight endoscope above and anterior to CNs VII and VIII provided a view of the abducens nerve entering the dura, the AICA origin from the basilar artery, and the a1 and a2 (Fig. 2J). The facial and cochlear nerves hidden anterior to the superior and inferior vestibular nerves are seen after drilling the posterior meatal wall (Fig. 3C).

The 45^{o} endoscope advanced above or below CN VIII and turned in various directions provided excellent views of the superior and inferior surfaces of CNs VII and VIII and their relationships at the brain stem and at the meatal porus. Angled endoscopes also provided superior views of the nervus intermedius, the a2, and the subarcuate, recurrent perforating, and

labyrinthine arteries (Fig. 2C to H). Advancing the endoscope anterior to CNs VII and VIII provided a view of the entire intradural course of the abducens nerve (Fig. 2J to M). Directing the 45^{o} scope laterally, after drilling the posterior wall of the meatus, exposed the individual nerves and the transverse and vertical crests at the meatal fundus (Fig. 3D and F). Directing the 45^{o} scope medially provides an excellent view of CNs VII and VIII at the lateral end of the potomedullary sulcus and slightly above the lower edge of the choroid plexus and flocculus protruding from the foramen of Luschka.

Lower Complex

The lower neurovascular complex includes the PICA, medulla, inferior cerebellar peduncle, cerebellomedullary fissure, suboccipital surface of the cerebellum, and the glossopharyngeal, vagus, spinal accessory, and hypoglossal nerves. The PICA, by definition, arises from the vertebral artery near the inferior olive and passes posteriorly around the medulla. At the anterolateral margin of the medulla, it passes rostral or caudal to or between the rootlets of the hypoglossal nerve, and at the posterolateral margin of the medulla it courses rostral to, or between, the fila of the glossopharyngeal, vagus, and accessory nerves. After passing the latter nerves, it courses on the inferior cerebellar peduncle and around the cerebellar tonsil to enter the cerebellomedullary fissure, and passes posterior to the lower half of the roof of the fourth ventricle. On exiting the cerebellomedullary fissure, its branches are distributed to the vermis and hemisphere of the suboccipital cerebellar surface. Most PICAs bifurcate into a medial and lateral trunk. The medial trunk supplies the vermis and adjacent part of the hemisphere, and the lateral trunk supplies the cortical surface of the tonsil and the hemisphere. The PICA has the most complex relationship to the cranial nerves of any artery. The proximal part of the PICA

passes around or between and often stretches or distorts the rootlets of the glossopharyngeal, vagus, accessory, and hypoglossal nerves.

The glossopharyngeal nerve arises as one or rarely two rootlets posterior to the superior third of the olive, just inferior to the pontomedullary junction and anterior to the foramen of Luschka and the rhomboid lip of the lateral recess of the fourth ventricle. The vagus nerve arises inferior to the glossopharyngeal nerve as a line of tightly packed rootlets posterior to the superior third of the olive. The accessory nerve arises as a widely separated series of rootlets that originates from the medulla and upper cervical cord, inferior to the vagus nerve below the level of the junction of the upper and middle third of the olive. The glossopharyngeal and vagus nerves arise rostral to the level of origin of the hypoglossal rootlets. The accessory rootlets arise at both the level of and inferior to the origin of the hypoglossal rootlets. The rootlets forming the hypoglossal nerve exit the medulla along the anterior margin of the caudal two-thirds of the olive along a line that is continuous inferiorly with the line along which the ventral spinal roots arise. The hypoglossal rootlets course anterolateral through the subarachnoid space and pass behind the vertebral artery to reach the hypoglossal canal.

PICA segments

The PICA is divided into 5 segments: (35)

Anterior Medullary Segment, p1. This segment lies anterior to the medulla. It begins at the origin of the PICA anterior to the medulla and extends backward past the hypoglossal rootlets to the level of a rostrocaudal line through the most prominent part of the inferior olive. The PICAs arising from the lower intradural part of the vertebral artery have no p1 segment because the vertebral artery at the origin of the PICA has not ascended to the front of the brain stem.

Lateral Medullary Segment, p2. This segment begins where the artery passes the most prominent point of the olive and ends at the level of the origin of the glossopharyngeal, vagus, and accessory rootlets.

Tonsillomedullary Segment, p3. This segment begins where the PICA passes posteriorly to the glossopharyngeal, vagus, and accessory nerves and extends medially across the posterior aspect of the medulla near the caudal half of the tonsil. It ends where the artery ascends to the midlevel of the medial surface of the tonsil. This segment forms a loop with a convex caudal curve called the caudal loop.

Telovelotonsillar Segment, p4. It begins at the midportion of the PICA's ascent along the medial surface of the tonsil toward the roof of the fourth ventricle and ends where it exits the fissures between the vermis, tonsil, and hemisphere to reach the suboccipital surface. This segment forms a loop with a convex rostral curve called the cranial loop.

Cortical Segment, p5. The cortical branches forming this segment radiate outward from the tonsil to the remainder of the vermis and the hemisphere forming the suboccipital surface.

The hypoglossal rootlets, in their course from the preolivary sulcus to the hypoglossal canal, pass posterior to the vertebral artery, except in the rare instance in which they pass anterior to the artery. The vertebral artery courses from the lateral side of the inferior part of the medulla to the anterior surface of the superior part of the medulla. If the vertebral artery is elongated or tortuous and courses lateral to the olive, it stretches the hypoglossal rootlets dorsally over its posterior surface. The hypoglossal rootlets are frequently stretched around the origin and initial segment of the PICAs that arise at the level of the caudal two-thirds of the olive, in addition to being stretched posteriorly by the vertebral artery. The most common course is for the PICA to arise from the vertebral artery and pass directly posteriorly around or between the hypoglossal

rootlets. However, some PICAs will loop upward, downward, or laterally in front of the hypoglossal rootlets before passing posteriorly between or around them. After coursing posteriorly to the hypoglossal rootlets, the PICA encounters and passes between the rootlets of the glossopharyngeal, vagus, and accessory nerves that exit the brain stem along the posterior edge of the olive. The PICA may be ascending, descending, or passing laterally or medially or be involved in a complex loop that stretches and distorts these nerves as it passes between them. Of the 42 PICAs found in 50 cerebella in a previous study, 16 passed between the rootlets of the accessory nerve, 10 passed between the rootlets of the vagus nerve, 13 passed between the vagus and accessory nerves, 2 passed above the glossopharyngeal nerve between the latter nerve and the vestibulocochlear nerve, and 1 passed between the glossopharyngeal and vagus nerves (23).

Microscopic View

The transcondylar fossa approach was utilized to expose the lower neurovascular complex (Fig. 4A). This approach is not to be confused with the transcondylar approach that involves drilling the occipital condyle. The transcondylar fossa approach is an inferiorly positioned, suboccipital approach with its lower edge directed through the condylar fossa located above the occipital condyle. It might be considered an inferolateral retrosigmoid approach. An approach directed along this fossa exposes the posterior edge of the sigmoid sinus low in the posterior fossa. The condylar fossa is often the site of an emissary vein that continues through the bone to empty into the sigmoid sinus.

This approach provides a wide operative view of the cerebellomedullary cistern located between the lateral surface of the medulla oblongata and the dura covering the jugular foramen. This approach exposes the posterior surface of the lower cranial nerves, the origin of the PICA, if the PICA arises from the lower portion of the vertebral artery on the lateral side of the brain stem

near the dural entrance of the vertebral artery (Fig. 4A and I). The approach did not expose the origin of the PICA if it arose from the part of a vertebral artery that had passed to the front of the brain stem (Fig. 4J). It may be difficult to see the glossopharyngeal and vagal meati at the dural roof of the jugular foramen and to differentiate the glossopharyngeal rootlet or rootlets from the vagal rootlets in the lateral medullary cistern. The posterior surface of the junction of CNs IX and X with the medulla is seen after elevation of the choroid plexus and flocculus at the foramen of Luschka. This approach exposes the p2, p3, and p5 but not the p4, which commonly can be exposed only with extensive separation of the cranial pole of the tonsil from the adjacent cerebellum. Only a short distal part of the p1, if present, may be seen anterior to the hypoglossal nerve.

Endoscopic View

The 0^{o} endoscope, after elevation of the choroid plexus and flocculus behind CNs IX and X, provided satisfactory visualization of the entire posterior surface of the lower cranial nerves (Fig. 4B). The hypoglossal rootlets are seen anterior to the cranial rootlets of the accessory nerve. Advancing the 0^{o} endoscope anteriorly between the accessory rootlets provided excellent visualization of the full course of the hypoglossal nerve from brain stem to dura and the p2 (Figs. 4K and 5C, E, and F). The close relationship of the thin rootlets forming the glossopharyngeal, vagus, and cranial accessory nerves, restricts movement of the endoscope if advanced between these rootlets.

The 45^{o} endoscope provided superior views of the distal part of the lower cranial nerves at the dural roof of the jugular foramen where the glossopharyngeal and dural meati are located, the junction of CN IX to XII with the medulla, the choroid plexus at the foramen of Luschka, and the rhomboid lip, which is a pouch of neural tissue attached along the anterior margin of the

foramen of Luschka that sits on the posterior surface of CN IX (Fig. 4C, D, E, and H). It also provided excellent views of the full length of the hypoglossal rootlets from brain stem to their dural porus, and the segment of the vertebral artery passing adjacent or between the hypoglossal rootlets (Fig. 5A, B, and D).

The 45^{o} scope also provided a view of the origin of the p1 and p2 and their relationship to the inferior olive and the rootlets of CNs IX to XII (Figs. 4L and 5D). The 0 and 45^{o} scopes could be advanced to provide a view of the p3 coursing around the lower margin of the tonsil, the bifurcation of the PICA into medial and lateral trunks, and into the foramen of Magendie to expose the vagal and hypoglossal triangles in the lower part of the floor of the 4th ventricle (Fig. 4M to R). The p4 could usually be exposed only with extensive dissection because of its course deep in the cerebellomedullary fissure.

DISCUSSION

The use of the endoscope in the CPA was first reported in 1917 by Doyen who used it for trigeminal root section via a retrosigmoid craniotomy (6). There were no additional reports of use of the endoscope in the CPA until 1993 when O'Donoghue and O'Flynn documented the endoscopic anatomy of the CPA and divided the CPA into four levels, and Magnan et al. reported their adjunctive use of endoscopy during posterior surgery for acoustic tumor removal and neurovascular decompression (26,31). Magnum et al. later reported the use of the endoscope to assist microscopic vascular decompression of the facial nerve for hemifacial spasm, and noted an additional 72% accuracy rate in identifying vascular compression of CN VII (24,25). In 1999, Goksu et al. provided the first report of the removal of acoustic neuroma using only endoscopic visualization (11). Jarrahy et al. first reported one case of fully endoscopic vascular decompression of trigeminal nerve in 2002 (16). Other studies showed the importance of angled

endoscopes in identifying the compressing vessels in vascular decompression procedures (1,9,18,21). Charalampaki et al. showed that compression by the hidden part of small arteries and especially veins can be better visualized with an angled endoscope placed in front of the pathology because of the ability of the angled endoscopes to "look around the corner" and inside cavities like Meckel's cave or the internal auditory canal, which cannot be seen with "the straight line view" of the microscope (3). Additionally, the use of the endoscope reduced the need for cerebellar retraction while minimizing injury to neural and vascular structures.

In this study, we divided the CPA into three levels (superior, middle, and inferior) and evaluated the use of both the endoscopic and the microscopic approaches via the retrosigmoid route at all three levels.

Superior Level

The entire course of the trigeminal nerve in the microscopic view was frequently hidden deep to the tributaries of the superior petrosal vein or the protrusions of the petrous bone (Fig. 1I and J). In contrast, the endoscope provided a view (Fig. 1B-H and K-N) and access to all areas of the trigeminal nerve from pons to Meckel's cave with minimal retraction (17,18,25,31). The superior petrosal vein or some of its tributaries are often divided to gain adequate exposure of the trigeminal nerve under the microscope. Obstruction of these veins may cause hemorrhage, cerebellar swelling, and venous infarction (21). Endoscopes, especially the angled scopes, are helpful in seeing around these obstructions and preserving the superior petrosal veins and their tributaries while minimizing retraction. For vascular decompression of the trigeminal nerve, the endoscope has improved outcomes and reduced complications as compared to the microscope (18). In microvascular decompression (MVD) for TN, compressing vessels located near Meckel's cave, medial to the trigeminal nerve and deep to the overhanging wing of the

cerebellum, were often difficult to view with the microscope, thus resulting in incomplete identification of neurovascular compression, or incomplete decompression at the time of the operation. Lee et al. pointed out in their review of recurrent trigeminal neuralgia, that distally located veins near Meckel's cave were particularly difficult to see in dolichocephalic patients because the prominences of the petrous bone above the internal acoustic meatus obstruct the distal intradural course of the trigeminal nerve (22). Rak et al. also described large trigeminal veins compressing the trigeminal nerve and draining into the area of Meckel's cave that may be missed if the area is not carefully explored (32). They, furthermore, commented that the view of the 2 to 3 mm of trigeminal and facial nerves near the brain stem and the inferior and anterior surfaces of trigeminal nerve was greatly aided by the endoscope (32). Ebner et al. reported the retrosigmoid intradural suprameatal approach with the endoscope accessed medially located central skull base structures including the posterior part of the cavernous sinus (7). Notaris et al. explored the clival and petroclival area via the endoscopic retrosigmoid approach (5).

In this study, the microscope provided a satisfactory view of the posterior surface of the trigeminal nerve and the s2, and the s4 (Fig. 1A). The endoscope provides superior views of the trigeminal nerve's junction with the pons and entrance into the porus of Meckel's cave, the relationship of the trigeminal sensory root with the motor and aberrant sensory rootlets, the upper, lower, and medial sides of the trigeminal nerve, and the s1 and proximal s2 (Fig. 1H and O to T). Advancing the endoscope between the tentorium and trigeminal nerve accessed the lateral aspect of the interpeduncular cistern, and exposed CNs III and IV, the proximal SCA and PCA, the upper basilar and posterior communicating arteries, and the upper clival region (Fig. 1O-T).

Middle Level

Janetta et al., who first performed MVD for hemifacial spasm, noted that the arterial loop compressing the part of the facial nerve adjacent the brain stem may not be seen because of the protrusion of the flocculus or choroid plexus below the nerve (14). The root exit zone of the facial nerve is usually hidden laterally by the vestibulocochlear nerve and the flocculus, but this obstruction is overcome by the infraflocculer approach directed posterior to the glossopharyngeal nerve with elevation of the choroid plexus and flocculus.

Several authors have documented the efficacy of endoscope in MVD for hemifacial spasm. Eby et al. first reported three cases of fully endoscopic vascular decompression of facial nerve for hemifacial spasm in 2001. They found that the endoscopic view provided excellent panoramic views of the CPA and root exit zone of the facial nerve and allowed identification of vascular compression in all cases without brain retraction (8). Rak et al. noted that arterial compression at the root exit zone by small veins and arteries may be missed in hemifacial spasm patients (32).

King et al. demonstrated the value of endoscope-assisted surgery to treat acoustic neuroma, and noted that angled endoscopes permit exploration of the internal acoustic meatus with improved visualization of residual tumor and open air cells (20). Several authors have also reported that the endoscope was useful in avoiding over extensive drilling of the posterior portion of the internal acoustic meatus, and that it aided in hearing preservation during acoustic neuroma surgery (30) (36). Yuguang et al. also reported the endoscope increased the rate of complete removal of epidermoid tumors in the CPA and decreased the incidence of postoperative complications (38).

At this level, the microscope provided a satisfactory view of the posterior surface of the vestibulocochlear nerves and the meatal and postmeatal segments parts of the a2 (Fig. 2A). It

was somewhat difficult with the microscopic to see the root exit zone of the facial nerve from the brain stem and the entrance of the facial nerve into the porus of the internal auditory meatus, but the endoscope provided superior views of both areas (Fig. 2A and B to H). The endoscope also provided superior views of the medial side of CNs VII and XII, the a1 and a2, the relationship of nerve-related arteries to the nervus intermedius, facial and vestibulocochlear nerves, and the vascular relationships anterior to the CNs 7 and 8 (Fig. 2B to N).

Inferior Level

The transcondylar fossa approach was used to expose the lower neurovascular complex. This approach, directed above the occipital condyle through the transcondylar fossa and adjacent suboccipital area, provides an excellent view of the PICA, the vertebral artery, and the lower cranial nerves (13,19,29). Jarrahy et al., in the first fully endoscopic vascular decompression of the glossopharyngeal nerve, reported excellent visualization of the site of compression with minimal retraction of the surrounding structures (16). Ferroli et al. reported that the 30^{o} angled endoscope provided good visualization of the root entry zone of CNs IX and X (10).

We found, as have other authors, that the endoscope aided in identifying structures along the anterolateral brain stem (2,5,37). De Notaris et al. obtained a line of sight anterior to the brain stem by angling the endoscope inferomedially in the corridor between the dural porus of the hypoglossal canal and the rootlets of CNs X and XI (5). Movement of the endoscope to access caudally toward the foramen magnum and anteromedially was prevented by accessory nerve rootlets. The angled endoscope with a relatively sharp tip also had a risk of damaging the surrounding structures in this deep and narrow space.

In this study, the microscope provided satisfactory views of the posterior surface of the lower cranial nerves and the p2 arising from the mid-portion of the vertebral artery (Fig. 4A).

The endoscope provides superior views of the medullary junction and dural exit of the lower cranial nerves, the p1 arising anterior to the medulla near the vertebrobasilar junction, the p2 lateral to the medulla, and the p3 (Fig. 4D to H, and K and L). The endoscope provided a superior view of the vascular segments anterior to the lower cranial nerves (Figs. 4K to O and 5).

SUMMARY

In summary, the microscope provides a satisfactory view of the posterior surface of neural and vascular structures in the central part of the CPA cistern, but visualization of the proximal or distal parts of the intradural segment of the nerves was often reduced by overhanging cerebellar tissue and prominences along the posterior surface of the temporal bone. The angled endoscope, with its ability to see around corners and behind structures, facilitated exposure of the pori of Meckel's cave and the internal acoustic meatus, the glossopharyngeal and vagal meati at the roof of the jugular foramen, and the junction of nerves with the brain stem. The endoscope also provides superior views of the nerves and vessels coursing deep to CNs V and VII to XI including the oculomotor and trochlear nerves at the superior level, the abducens nerve at the middle level, and the hypoglossal nerve at the inferior level. In addition, the endoscope provides superior views of the vascular segments anterior to the nerves and the relationships of vessels to the nerves.

The major disadvantage of the endoscope is that it places a probe-like instrument in the operative field, which sees only from its tip and is largely hidden from view when the surgeon is focused on the endoscope image. This lack of backward or sideways vision makes it dangerous to move the endoscope in the operative field. Extreme care is needed to avoid allowing the endoscope to drift into and injure vessels and nerves located out of view along the side of the tube. The soft nature of the brain also necessitates that great care be taken to avoid the endoscope

slipping into and damaging the brain. This is especially true with the angled endoscope, which, when advance forward, does not see straight ahead. Also, the endoscopic images are 2-dimentional, not 3-dimentional, so the sense of depth may be lost. Considerable training is needed to attain the visuomotor skills needed to navigate using the endoscope among the vital structures in the CPA. These disadvantages are described by others (2,4,32). Furthermore, they have described developments in image fusion technology, instrumentation, holding devices, antifogging services, and irrigation devices needed to improve the usefulness of the endoscope (32).

CONCLUSION

The endoscope is useful as an adjacent instrument to the microscope in surgery for CPA lesions. The microscope provides a satisfactory view of the posterior surface of-neural and vascular structures in the central part of the CPA cistern. The endoscope provides superior views of the nerves from the brain stem to their dural exit, the individual segments of the cerebellar arteries, and the relationships of the nerves and arteries.

REFERENCES

1. Badr-El-Dine M, El-Garem HF, Talaat AM, Magnan J: Endoscopically assisted minimally invasive microvascular decompression of hemifacial spasm. Otol Neurotol 23:122-128, 2002.

2. Cappabianca P, Cavallo LM, Esposito F, de Divitiis E, Tschabitscher M: Endoscopic examination of the cerebellar pontine angle. Clin Neurol Neurosurg 104:387-391, 2002.

3. Charalampaki P, Kafadar AM, Grunert P, Ayyad A, Perneczky A: Vascular Decompression of Trigeminal and Facial Nerves in the Posterior Fossa under Endoscope-Assisted Keyhole Conditions. Skull Base 18:117-128, 2008.

4. Cheng WY, Chao SC, Shen CC: Endoscopic microvascular decompression of the hemifacial spasm. Surg Neurol 70 Suppl 1:S1:40-46, 2008.

5. de Notaris M, Cavallo LM, Prats-Galino A, Esposito I, Benet A, Poblete J, Valente V, Gonzalez JB, Ferrer E, Cappabianca P: Endoscopic endonasal transclival approach and retrosigmoid approach to the clival and petroclival regions. Neurosurgery 65:42-50; discussion 50-42, 2009.

6. Doyen E. *Surgical Therapeutics and Operative Techniques.* Vol 599-602. London: Balliere, Tindall, and Cox; 1917.

7. Ebner FH, Koerbel A, Roser F, Hirt B, Tatagiba M: Microsurgical and endoscopic anatomy of the retrosigmoid intradural suprameatal approach to lesions extending from the posterior fossa to the central skull base. Skull Base 19:319-323, 2009.

8. Eby JB, Cha ST, Shahinian HK: Fully endoscopic vascular decompression of the facial nerve for hemifacial spasm. Skull Base 11:189-197, 2001.

9. El-Garem HF, Badr-El-Dine M, Talaat AM, Magnan J: Endoscopy as a tool in minimally invasive trigeminal neuralgia surgery. Otol Neurotol 23:132-135, 2002.

10. Ferroli P, Fioravanti A, Schiariti M, Tringali G, Franzini A, Calbucci F, Broggi G: Microvascular decompression for glossopharyngeal neuralgia: a long-term retrospectic review of the Milan-Bologna experience in 31 consecutive cases. Acta Neurochir (Wien) 151:1245-1250, 2009.

11. Goksu N, Bayazit Y, Kemaloglu Y: Endoscopy of the posterior fossa and endoscopic dissection of acoustic neuroma. Neurosurg Focus 6:e15, 1999.

12. Hardy DG, Rhoton AL, Jr.: Microsurgical relationships of the superior cerebellar artery and the trigeminal nerve. J Neurosurg 49:669-678, 1978.

13. Hitotsumatsu T, Matsushima T, Inoue T: Microvascular decompression for treatment of trigeminal neuralgia, hemifacial spasm, and glossopharyngeal neuralgia: three surgical approach variations: technical note. Neurosurgery 53:1436-1441; discussion 1442-1433, 2003.

14. Jannetta PJ, Abbasy M, Maroon JC, Ramos FM, Albin MS: Etiology and definitive microsurgical treatment of hemifacial spasm. Operative techniques and results in 47 patients. J Neurosurg 47:321-328, 1977.

15. Jarrahy R, Berci G, Shahinian HK: Endoscope-assisted microvascular decompression of the trigeminal nerve. Otolaryngol Head Neck Surg 123:218-223, 2000.

16. Jarrahy R, Eby JB, Cha ST, Shahinian HK: Fully endoscopic vascular decompression of the trigeminal nerve. Minim Invasive Neurosurg 45:32-35, 2002.

17. Jennings CR, O'Donoghue GM: Posterior fossa endoscopy. J Laryngol Otol 112:227-229, 1998.

18. Kabil MS, Eby JB, Shahinian HK: Endoscopic vascular decompression versus microvascular decompression of the trigeminal nerve. Minim Invasive Neurosurg 48:207-212, 2005.

19. Kawashima M, Matsushima T, Inoue T, Mineta T, Masuoka J, Hirakawa N: Microvascular decompression for glossopharyngeal neuralgia through the transcondylar fossa (supracondylar transjugular tubercle) approach. Neurosurgery 66:275-280; discussion 280, 2010.

20. King WA, Wackym PA: Endoscope-assisted surgery for acoustic neuromas (vestibular schwannomas): early experience using the rigid Hopkins telescope. Neurosurgery 44:1095-1100; discussion 1100-1092, 1999.

21. King WA, Wackym PA, Sen C, Meyer GA, Shiau J, Deutsch H: Adjunctive use of endoscopy during posterior fossa surgery to treat cranial neuropathies. Neurosurgery 49:108-115; discussion 115-106, 2001.

22. Lee SH, Levy EI, Scarrow AM, Kassam A, Jannetta PJ: Recurrent trigeminal neuralgia attributable to veins after microvascular decompression. Neurosurgery 46:356-361; discussion 361-352, 2000.

23. Lister JR, Rhoton AL, Jr., Matsushima T, Peace DA: Microsurgical anatomy of the posterior inferior cerebellar artery. Neurosurgery 10:170-199, 1982.

24. Magnan J, Caces F, Locatelli P, Chays A: Hemifacial spasm: endoscopic vascular decompression. Otolaryngol Head Neck Surg 117:308-314, 1997.

25. Magnan J, Chays A, Lepetre C, Pencroffi E, Locatelli P: Surgical perspectives of endoscopy of the cerebellopontine angle. Am J Otol 15:366-370, 1994.

26. Magnan J, Chays A, Caces F, Lepetre C, Cohen JM, Belus JF, Bruzzo M: [Contribution of endoscopy of the cerebellopontine angle by retrosigmoid approach. Neuroma and vasculo-nervous compression]. Ann Otolaryngol Chir Cervicofac 110:259-265, 1993.

27. Martin RG, Grant JL, Peace D, Theiss C, Rhoton AL, Jr.: Microsurgical relationships of the anterior inferior cerebellar artery and the facial-vestibulocochlear nerve complex. Neurosurgery 6:483-507, 1980.

28. Matsushima T, Rhoton AL, Jr., de Oliveira E, Peace D: Microsurgical anatomy of the veins of the posterior fossa. J Neurosurg 59:63-105, 1983.

29. Matsushima T, Natori Y, Katsuta T, Ikezaki K, Fukui M, Rhoton AL: Microsurgical anatomy for lateral approaches to the foramen magnum with special reference to transcondylar fossa (supracondylar transjugular tubercle) approach. Skull Base Surg 8:119-125, 1998.

30. Matula C, Diaz Day J, Czech T, Koos WT: The retrosigmoid approach to acoustic neurinomas: technical, strategic, and future concepts. Acta Neurochir (Wien) 134:139-147, 1995.

31. O'Donoghue GM, O'Flynn P: Endoscopic anatomy of the cerebellopontine angle. Am J Otol 14:122-125, 1993.

32. Rak R, Sekhar LN, Stimac D, Hechl P: Endoscope-assisted microsurgery for microvascular compression syndromes. Neurosurgery 54:876-881; discussion 881-873, 2004.

33. Rhoton AL, Jr.: The cerebellar arteries. Neurosurgery 47:S29-68, 2000.

34. Rhoton AL, Jr.: The cerebellopontine angle and posterior fossa cranial nerves by the retrosigmoid approach. Neurosurgery 47:S93-129, 2000.

35. Rodriguez-Hernandez A, Rhoton AL, Jr., Lawton MT: Segmental anatomy of cerebellar arteries: a proposed nomenclature. Laboratory investigation. J Neurosurg 115:387-397, 2011.

36. Samii M, Matthies C, Tatagiba M: Management of vestibular schwannomas (acoustic neuromas): auditory and facial nerve function after resection of 120 vestibular schwannomas in patients with neurofibromatosis 2. Neurosurgery 40:696-705; discussion 705-696, 1997.

37. Xia Y, Li XP, Han DM, Zheng J, Long HS, Shi JF: Anatomic structural study of cerebellopontine angle via endoscope. Chin Med J (Engl) 120:1836-1839, 2007.

38. Yuguang L, Chengyuan W, Meng L, Shugan Z, Wandong S, Gang L, Xingang L: Neuroendoscopic anatomy and surgery of the cerebellopontine angle. J Clin Neurosci 12:256-260, 2005.

FIGURE LEGENDS

Figure 1. A, upper part of right CPA as seen through the surgical microscope in the lateral infratentorial approach in the sitting position. The cisternal part of the posterior surface of the trigeminal nerve is exposed. The entry of the nerve into the porus of Meckel's cave and the posterior surface of the root exit zone are not as well seen as with the endoscope. The s2 compresses the rostromedial side of the posterior root. A superior petrosal vein and the distal segments (s3 and s4) of the SCA limit access to the nerve. **B,** the 0^{o} endoscopic view without retraction. It provided a view of the entire course of the trigeminal nerve from the pons to Meckel's cave. C to H, endoscopic views of the same specimen. **C,** 45^{o} angled medially and slightly downward showing the junction of the trigeminal nerve with the pons. The s2 and junction of the trigeminal nerve with the brain stem are seen much better with the endoscope. The s2 courses medial to and compresses the rostromedial side of the trigeminal root. **D,** 45^{o} angled medially below the trigeminal nerve showing the compressing s2 looping below the caudal edge of the nerve. This loop below the nerve was not seen with the microscope. **E,** 45^{o} angled laterally showing the superior surface of the right trigeminal nerve entering Meckel's cave. **F,** 45^{o} angled upward showing the inferior surface of the trigeminal nerve entering Meckel's cave. **G,** 45^{o} angled laterally showing the anterior surface of the right trigeminal nerve entering Meckel's cave. A superior petrosal vein is seen entering the dura along the antero-inferior surface of the nerve near Meckel's cave. A branch of the s2 rests against the anterior side of the nerve near Meckel's cave. **H,** 45^{o} angled lateral. Four motor rootlets are exposed above the sensory root. A small aberrant rootlet arises from the pons above the main sensory root and joins the sensory root about 1 cm from the brain stem. I to N, comparison of the microscopic (I and J) and the endoscopic views (K to N) of the left trigeminal nerve in two additional CPAs. I and K

are from one CPA, J and L to N are from another. **I,** the suprameatal tubercle located above the porus of the internal acoustic meatus obscures the microscopic view of the part of the trigeminal nerve adjacent Meckel's cave. **J,** two large petrosal veins and the suprameatal tubercle block the microscope view of the trigeminal nerve. **K,** 45^{o} angled upward. The caudal trunk of the s2 courses below the rostral trunk and compresses the superomedial aspect of CN V. L to N, 0^{o} endoscopic views. **L,** superior petrosal veins pass along the lateral and upper surface of CN V. **M,** the s2 passes above the upper superior petrosal vein and a branch of the s4 segment passes above CN V. **N,** two petrosal veins and the s2 are in the exposure. A branch of the a4 loops up lateral to the trigeminal nerve. O to R, left side, 45^{o} angled upward. Endoscopic views of the oculomotor and trochlear nerves and surrounding structures. **O,** the s1 and s2 are seen adjacent the trochlear and the oculomotor nerves. **P,** enlarged view. The oculomotor nerve passes below the uncus, and the trochlear nerve enters the tentorial edge. The posterior cerebral (P2) and posterior communicating arteries, and the s1 are exposed adjacent CN III. **Q,** CN III passes below the uncus and P2 and above the posterior communicating artery. **R,** view below the posterior communicating artery. The dorsum sellae, midline clivus, and the basilar, posterior communicating, and premamillary arteries are exposed. S and T, right side, 45^{o} upward. **S,** the anterior surface of the basilar artery and the floor of the 3^{rd} ventricle are exposed between the ipsilateral and contralateral posterior communicating arteries. **T,** enlarged view. The mamillary bodies are exposed above the basilar artery and P1.The tuber cinereum can be seen through Liliequist's membrane. A., artery; Bas., basilar; Caud., caudal; Cer., cerebellar; Cin., cinereum; Clin., clinoid; CN, cranial nerve; Contra., contralateral; Ipsi., ipsilateral; Mam., mamillary; Memb., membrane; P.Co.A., posterior communicating artery; Pet., petrosal; Post., posterior;

Premam., premamillary; Rost., rostral; Sup., superior; Suprameat., suprameatal; Tent., tentorium; Tr., Trunk; V., vein; Vent., ventricle.

Figure 2. A, middle complex in the CPA as seen in the lateral suboccipital infrafloccular approach through the operating microscope in the sitting position. The flocculus and choroid plexus have been retracted upward to expose the root exit zone of the facial nerve below the vestibulocochlear nerve. The premeatal segment of the AICA is hidden anterior to CN VIII and the postmeatal segment is seen after it has passed between CNs VII and VIII. The subarcuate, labyrinth, and recurrent perforating arteries originate from the meatal segment of the a2. **B,** 0^{o} endoscopic view provides a view of entire posterior surface of the vestibulocochlear nerve from the brain stem to the porus of the auditory meatus. The proximal part of CN VII is exposed anterior inferior to CN VIII. **C,** 45^{o} angled medially. The junction of the left facial nerve with the brain stem is located below and slightly in front of the vestibulocochlear nerve. Choroid plexus protrudes from the foramen of Luschka into the cerebellopontine angle behind the glossopharyngeal and vagus nerves. The facial and vestibulocochlear nerves join the brain stem at the lateral end of the pontomedullary sulcus, anterior to the flocculus, rostral to the glossopharyngeal, vagus, and accessory nerves, and anterosuperior to the choroid plexus protruding from the foramen of Luschka. **D,** enlarged view of C. The nervus intermedius arises at the brain stem along the anterior surface of the vestibulocochlear nerve and joins the facial nerve distally. **E,** 45^{o} angled downward exposes the superior surface of the junction of the facial and vestibulocochlear nerves with the brain stem and an a2 coursing between CNs VII and VIII. **F,** 45^{o} angled lateral. The vestibulocochlear nerve enters the internal acoustic meatus with a labyrinthine branch of the a2. The subarcuate artery enters the dura on the posterior wall of the internal acoustic meatus. **G,** 45^{o} angled upward below CNs VII and VIII. The a2 gives rise to a

recurrent perforating branch to the brain stem. The premeatal and meatal segments of the a2 and the subarcuate, labyrinthine, and recurrent perforating arteries are seen below CNs VII and VIII. **H,** 45° angled downward above the superior surface of CNs VII and VIII. The a2 passes between the facial and vestibulocochlear nerves and also between several rootlets forming the nervus intermedius. I to M, endoscopic view of the left abducens nerve and surrounding structures. I and J, sitting position. **I,** 0° endoscope. The abducens nerve and the a1 are exposed deep to CNs VIII and IX. **J,** the endoscope has been advanced between CNs V and VIII to expose the abducens nerve ascending anterior to the pons and the a1. **K,** three-quarter prone position, 45° angled caudally. The entire course of the abducens nerve from the pontomedullary junction to its dural entrance is exposed. The a1 passes above CN VI. **L,** another specimen, 45° angled upward. The a1 passes below CN VI and bifurcates to form an a2 having a rostral and a caudal trunk. **M,** another specimen, 45°angled upward. The abducens nerve is stretched over the rostral surface of the ipsilateral vertebral artery. The proximal part of the a1 crosses the upper surface of the abducens nerve. **N,** the a1 arises from the basilar artery and courses between the clivus and pons. A., artery; A.I.C.A., anteroinferior cerebellar artery; Bas., basilar; Caud., caudal; Cer., cerebellar; Chor., choroidal; CN, cranial nerve; Contra., contralateral; Flocc., flocculus; For., foramen; Intermed., intermedius; Ipsi., ipsilateral; Labyr., labyrinthine; Meat., meatal; Mid., middle; Nerv., nervus; Ped., peduncle; Perf., perforating; Pet., petrosal; Plex., plexus; Postmeat., postmeatal; Premeat., premeatal; Rec., recurrent; Rost., rostral; Seg., segment; Subarc., subarcuate; Sup., superior; Tr., Trunk; V., vein; Vert., vertebral.

Figure 3. A to F; microscopic (A, B, and E) and endoscopic (C, D, and F) views of the internal acoustic meatus. **A,** cerebellopontine angle exposed by left retrosigmoid approach. The posterior meatal wall has been removed to expose the dura lining the meatus. **B,** the dura lining

the internal acoustic meatus has been opened. The transverse crest separates the superior vestibular and facial nerves above from the inferior vestibular and cochlear nerves below. The facial and cochlear nerves are partially hidden anterior to the superior and inferior vestibular nerves. **C,** 0°angled view. The cleavage plane between the superior and inferior vestibular and cochlear nerves has been started laterally and extended medially to expose the individual nerves. **D,** 45°angled view directed upward toward the lower surface of the nerves. The vertical and transverse crests are exposed at the meatal funds. **E,** view of the right internal acoustic meatus exposed by the retrosigmoid approach. The common crus and adjacent part of the superior and posterior canals have been exposed. The endolymphatic sac is situated in the dura inferolateral to the internal acoustic meatus. **F,** 45° angled laterally toward the fundus of the meatus. CN, cranial nerve; Coch., cochlear; Endolymph., endolymphatic; Inf., inferior; Intermed., intermedius; N., nerve; Nerv., nervus; P.I.C.A., posteroinferior cerebellar artery; Post., posterior; Sup., superior; Trans., transverse; Vert., vertebral; Vest., vestibular.

Figure 4. A, lower complex in the CPA as seen in the transcondylar fossa approach through the surgical microscope. The flocculus and choroid plexus have been elevated to expose the posterior surface of the rootlets forming CNs IX, X, and XI. **B,** 0 ° endoscope. It provides a view of the entire posterior surface of CNs IX, X, and XI from medulla to the dural meati. **C,** 45° angled laterally toward the dural roof of the jugular foramina where the glossopharyngeal, vagus and accessory nerves enter the shallow dural glossopharyngeal and vagal meati. The glossopharyngeal and vagus nerves are consistently separated by a dural septum at the level of the roof over the jugular foramen. The jugular dural fold projects downward and medially over the lateral edge of the glossopharyngeal and vagal meati. D to H, endoscopic views of the nerves joining the brain stem. **D,** 45° angled medially. CNs IX, X, and XI arise as a line of rootlets that

exit the brain stem along the posterior edge of the olive in the post-olivary sulcus. The rhomboid lip projects laterally from the ventral margin of the foramen of Luschka behind CNs IX and X. **E,** 45^{o} angled medially. CN IX arises as a single rootlet from the upper medulla and just caudal to the origin of the facial nerve. The vagus nerve arises inferior to the glossopharyngeal nerve as a line of tightly packed rootlets posterior to the superior third of the olive. The hypoglossal rootlets are stretched around the origin of a PICA that arises as a p2 on the lateral side of the medulla **F,** 0^{o} directed medially. The accessory nerve arises from the medulla as a widely separated series of rootlets posterior to the level of the lower two-thirds of the olive, and from the upper cervical cord. The hypoglossal nerve arises as a line of rootlets that exit the brain stem along the anterior margin of the caudal two-thirds of the olive and anterior to the accessory rootlets. **G,** 0^{o} looking upward. The C1 nerve rootlets pass through the dura with the vertebral artery. The dentate ligament ascends anterior and the accessory nerve posterior to the vertebral artery. A posterior spinal artery arises from the PICA and courses along the dorsolateral aspect of the spinal cord. **H,** another specimen, right side, 45^{o} angled medially and upward along the caudal edge of CN X. The choroid plexus projects laterally from the foramen of Luschka into the CPA behind CNs VIII and IX. The rhomboid lip projects laterally along the anterior margin of the foramen of Luschka. I to L, comparison of microscopic (I and J) and endoscopic views (K and L) of the PICA origin along the anterolateral medulla. **I,** the left p2 arises along the lateral side of the medulla from the mid-portion of the vertebral artery. Some hypoglossal rootlets are stretched around the upper margin of the PICA origin. P3 and p5 are seen but p4 is hidden anterior to the tonsil. **J,** microscopic view. A right p1 is present but not seen because it arises on the anterior side of the medulla. **K,** 0^{o} directed upward. The PICA origin stretches the hypoglossal rootlets rostrally. There is no p1 because the PICA arises as a p2 lateral to the brain stem. **L,** 45^{o} angled

upward showing the PICA origin anterior to the brain stem shown in J. M to R, 0^{o} directed upward showing endoscopic views of the segments of the PICA (left side). **M,** this PICA arises lateral to the medulla and does not have a p1. **N,** the p2 passes caudally in front of CNs X and XI and then turns dorsally between the rootlets of CN XI to reach the posterolateral medulla to enter the cerebellomedullary fissure. The p4 passes medially to enter the cerebellomedullary fissure. **O,** the p3 begins where the PICA passes posterior to the CN IX to XI and courses along the posterolateral medulla and inferior cerebellar peduncle to enter the cerebellomedullary fissure. **P,** the p3 extends medially across the posterior aspect of the medulla and commonly forms a caudal loop at the lower pole of the cerebellar tonsil. The p4 begins at the midlevel of the PICA's ascent along the medial surface of the tonsil in the cerebellomedullary fissure. The p5 begins where the trunks exit the cerebellomedullary fissure and is composed of the cortical branches supplying the suboccipital cerebellar surface. **Q,** the p4 has been exposed in the cerebellomedullary fissure by retracting the tonsil. The p4 ends where it exits the fissures between the vermis, tonsil, and hemisphere to give rise to the p5, which commonly divides into a medial trunk that supplies the vermis and adjacent part of the hemisphere, and a caudal trunk that loops around the tonsil to supply the largest part of the hemispheric surface. **R,** view of the foramen of Magendie. The hypoglossal and vagal nuclei are in the lower part of the floor of the 4^{th}ventricle. The p4 enters the cerebellomedullary fissure.

A., artery; Atl., atlanto; Br., branch; Bridg., bridging; Cer., cerebellar, cerebral; Chor., choroid, choroidal; CN, cranial nerve; Cond., condyle, condylar; Dent., dentate; Fiss., fissure; Glossophar., glossopharyngeal; Hypogl., hypoglossal; Inf., inferior; Jug., jugular; Lat., lateral; Lig., ligament; Med., medial, medularis, medullary; Mid., middle; Occip., occipital; Ped.,

peduncle; P.I.C.A., posteroinferior cerebellar artery; Plex., plexus; Post., posterior; Sp., spinal; Tr., Trunk; V., vein; Verm., vermian; Vert., vertebral.

Figure 5. A to F. Endoscopic views of the hypoglossal nerve and surrounding vascular structures. **A,** right side, 45^{o} lateral. The hypoglossal nerve arises as a line of rootlets that exit the brain stem along the anterior margin of the lower two-thirds of the olive in the preolivary sulcus. The hypoglossal rootlets collect into three separate bundles as they enter the dura. **B,** left side, 45^{o} lateral. The vertebral artery passes between the rootlets of the hypoglossal nerve. The hypoglossal rootlets collect into two bundles before entering the dura. **C,** left side, 0^{o} upward. The hypoglossal rootlets pass behind the vertebral artery to reach the hypoglossal canal. **D,** left side, 45^{o} caudally. The hypoglossal rootlets pass anterior to the vertebral artery. The PICA arises caudal to the olive and posterior to the hypoglossal rootlets. The p3 begins where the artery passes dorsal to CN IX, X, and XI. **E,** right side, 0^{o} upward. The vertebral artery is straight and does not contact or distort the hypoglossal rootlets as do many PICAs. **F,** left side, 0^{o} upward. The vertebral artery is tortuous, courses laterally to the olive and stretches the hypoglossal rootlets over its posterior surface. The hypoglossal rootlets are stretched rostrally around the origin of the PICA. The PICA arises as a p2 lateral to the brain stem. A., artery; Bridg., bridging; CN, cranial nerve; P.I.C.A., posteroinferior cerebellar artery; Post., posterior; Sp., spinal; V., vein; Vert., vertebral.

Figure 1A-D

Click here to download high resolution image

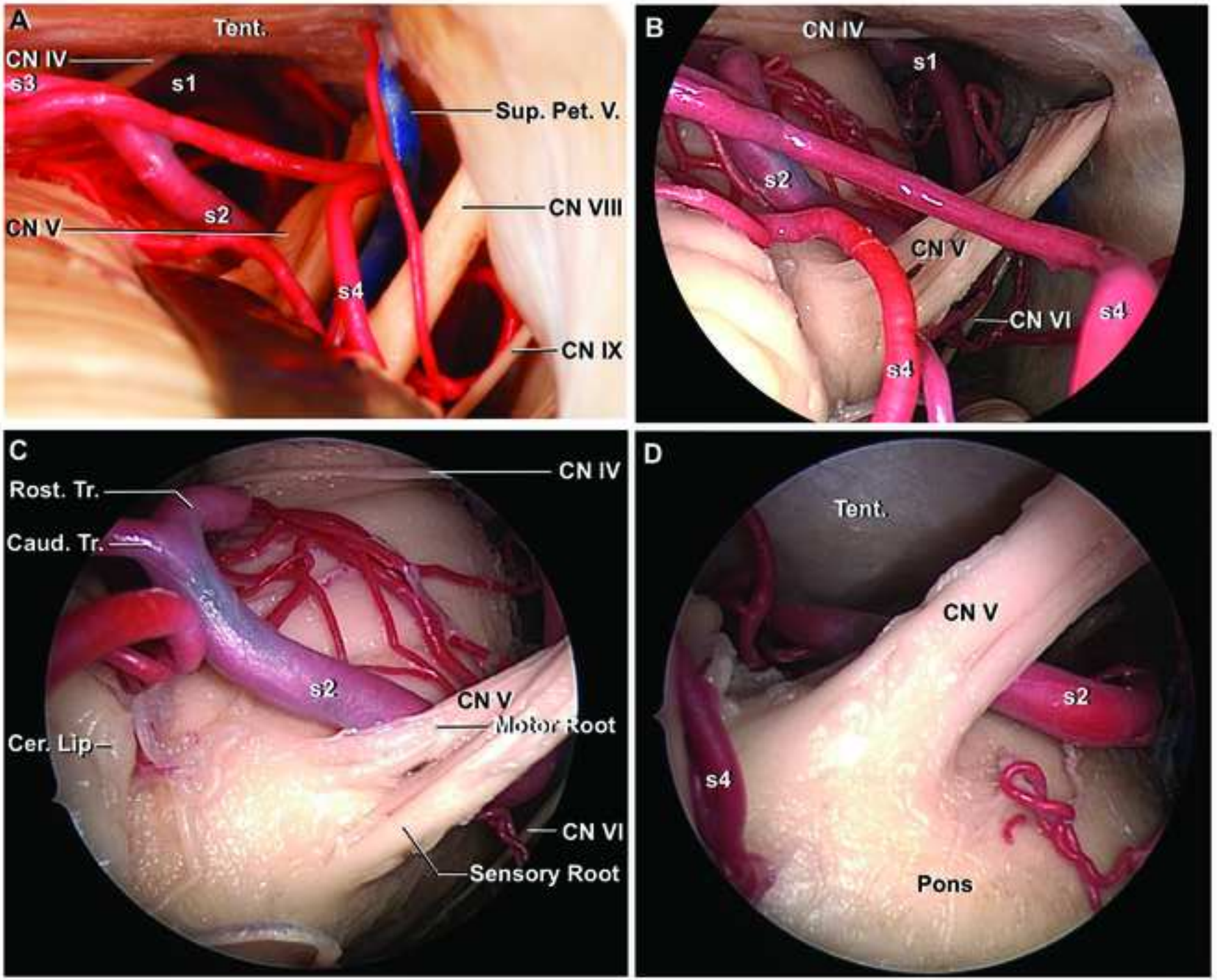

Figure 1E-H

Click here to download high resolution image

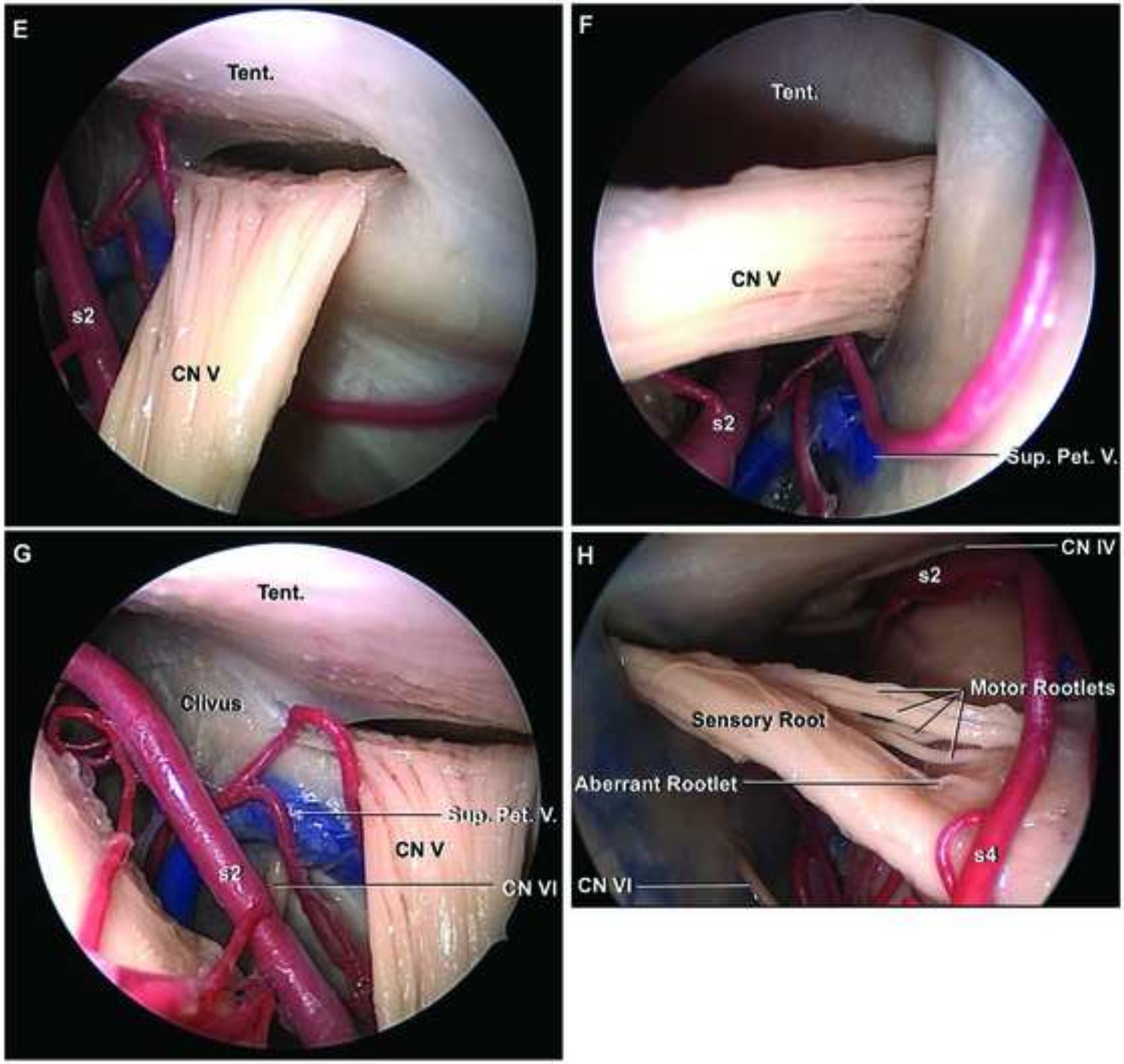

Figure 1I-N

Click here to download high resolution image

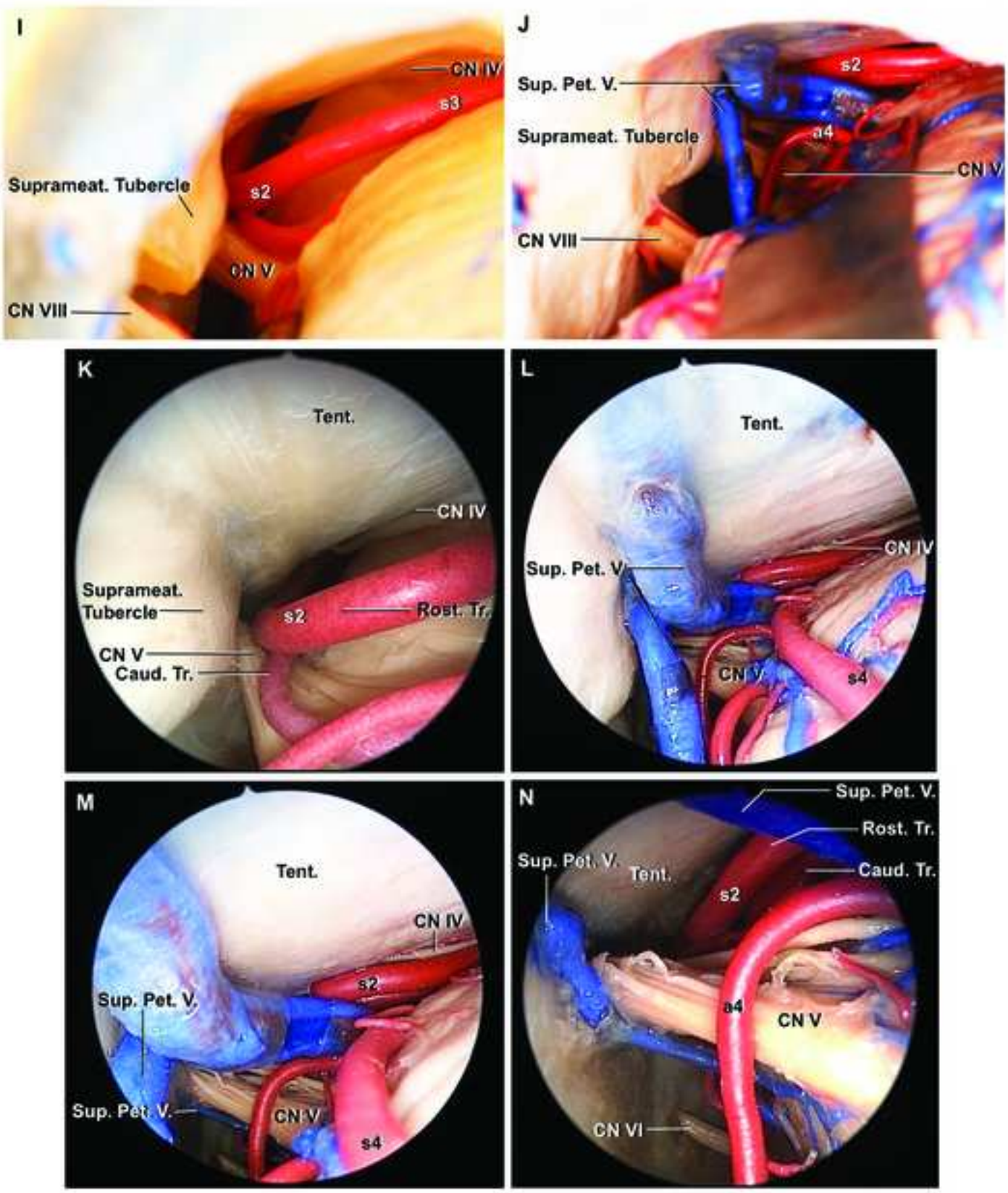

Figure 1O-T

Click here to download high resolution image

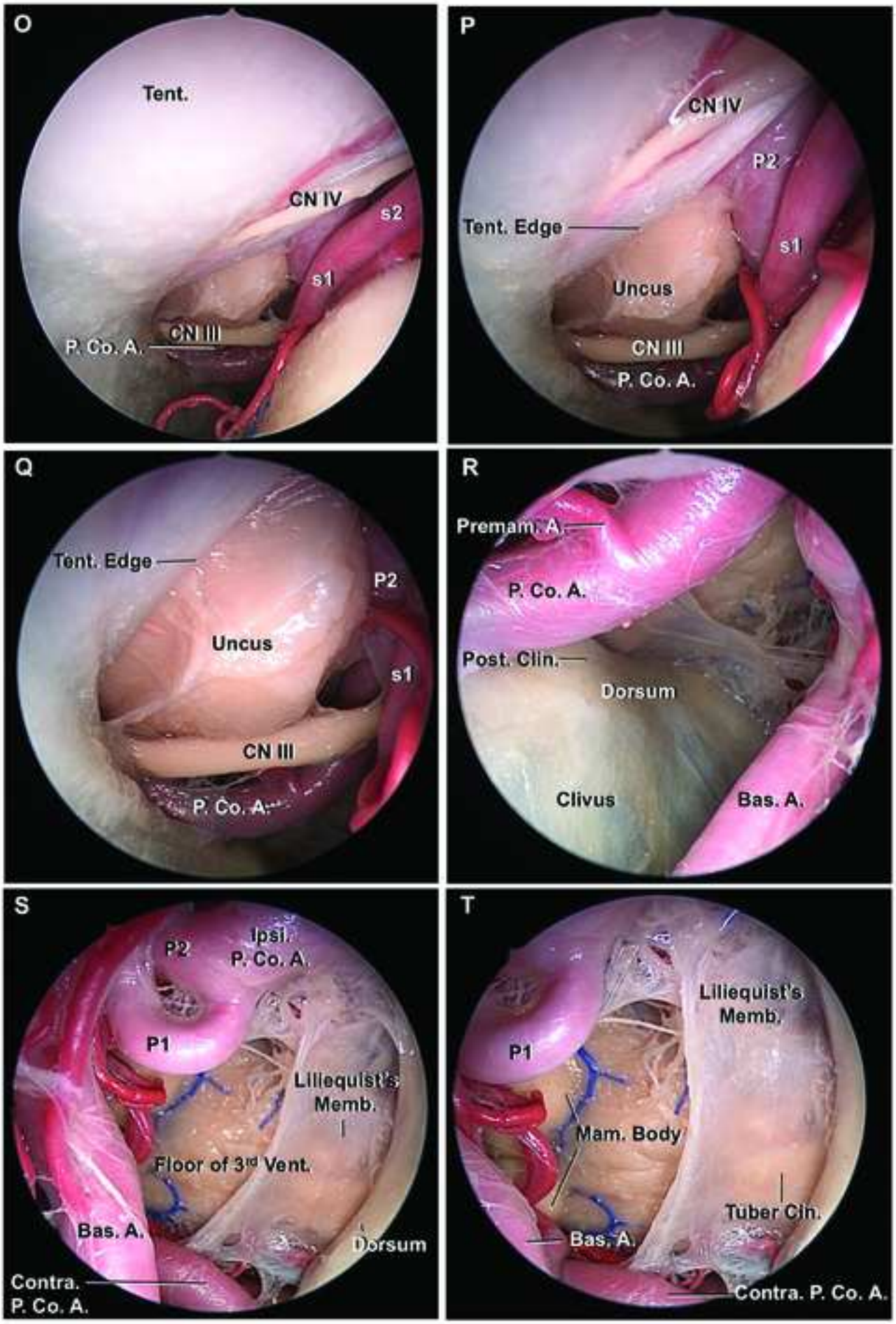

Figure 2A-D

Click here to download high resolution image

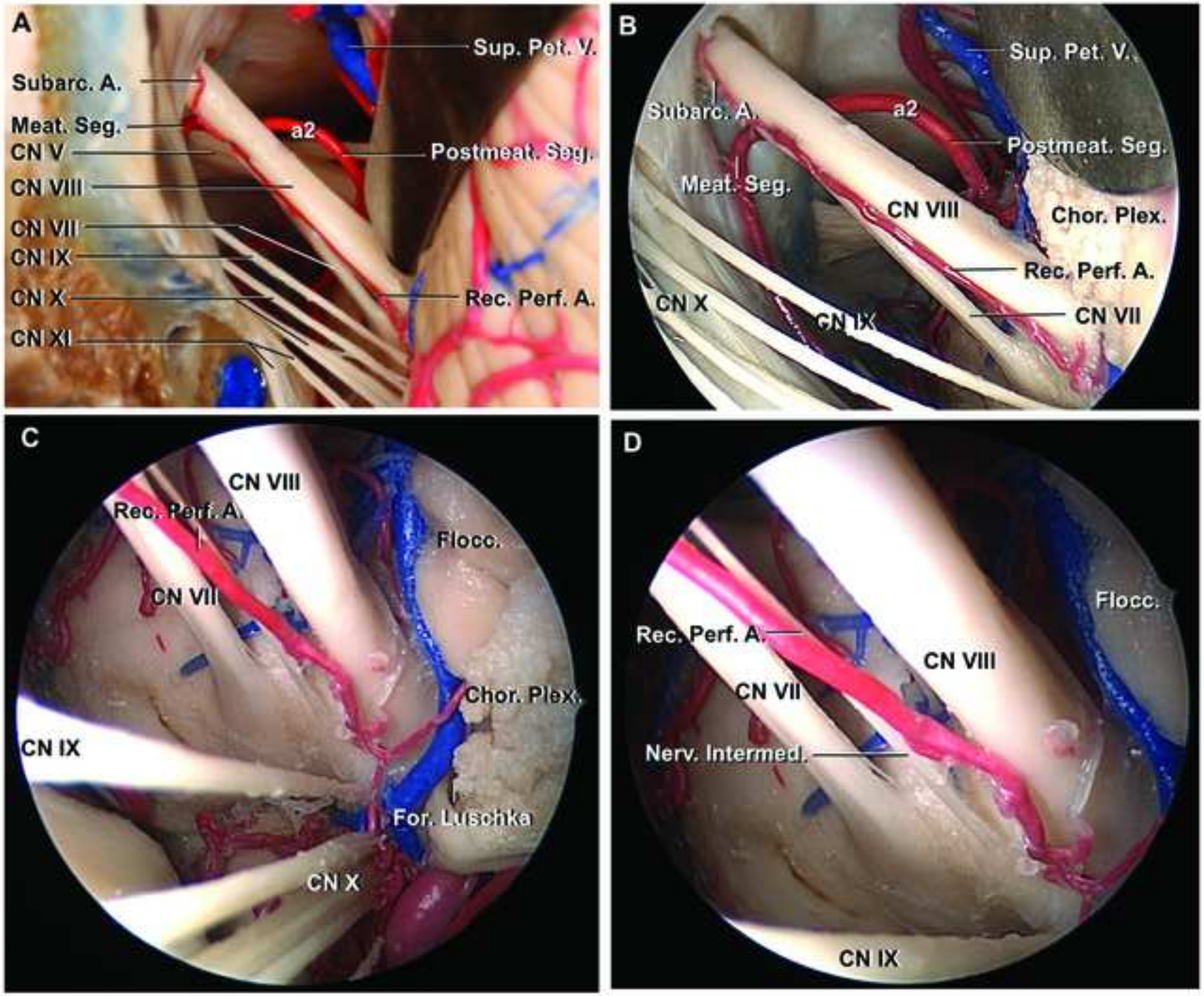

Figure 2E-H

Click here to download high resolution image

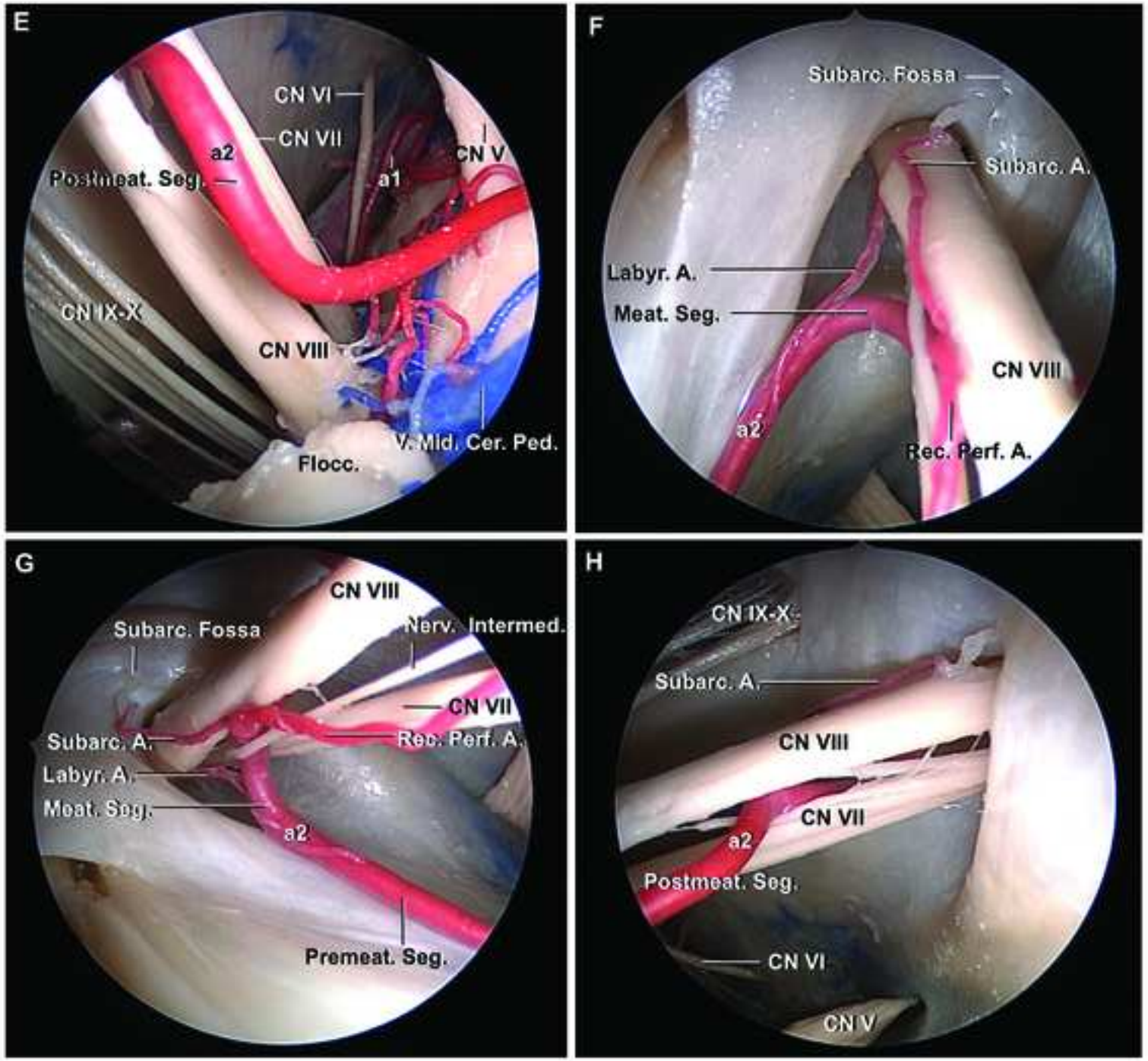

Figure 2I-N

Click here to download high resolution image

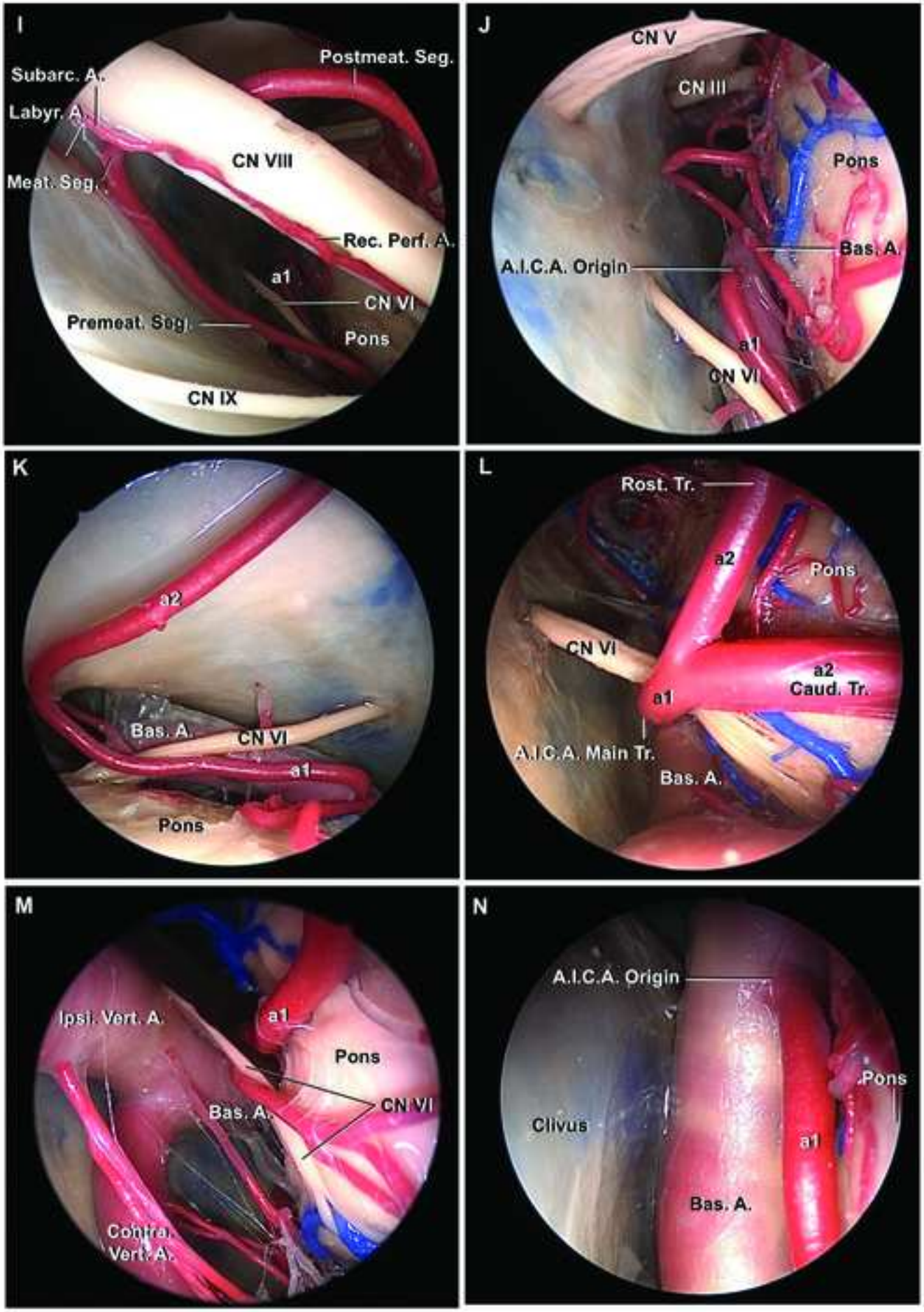

Figure 3A-F

Click here to download high resolution image

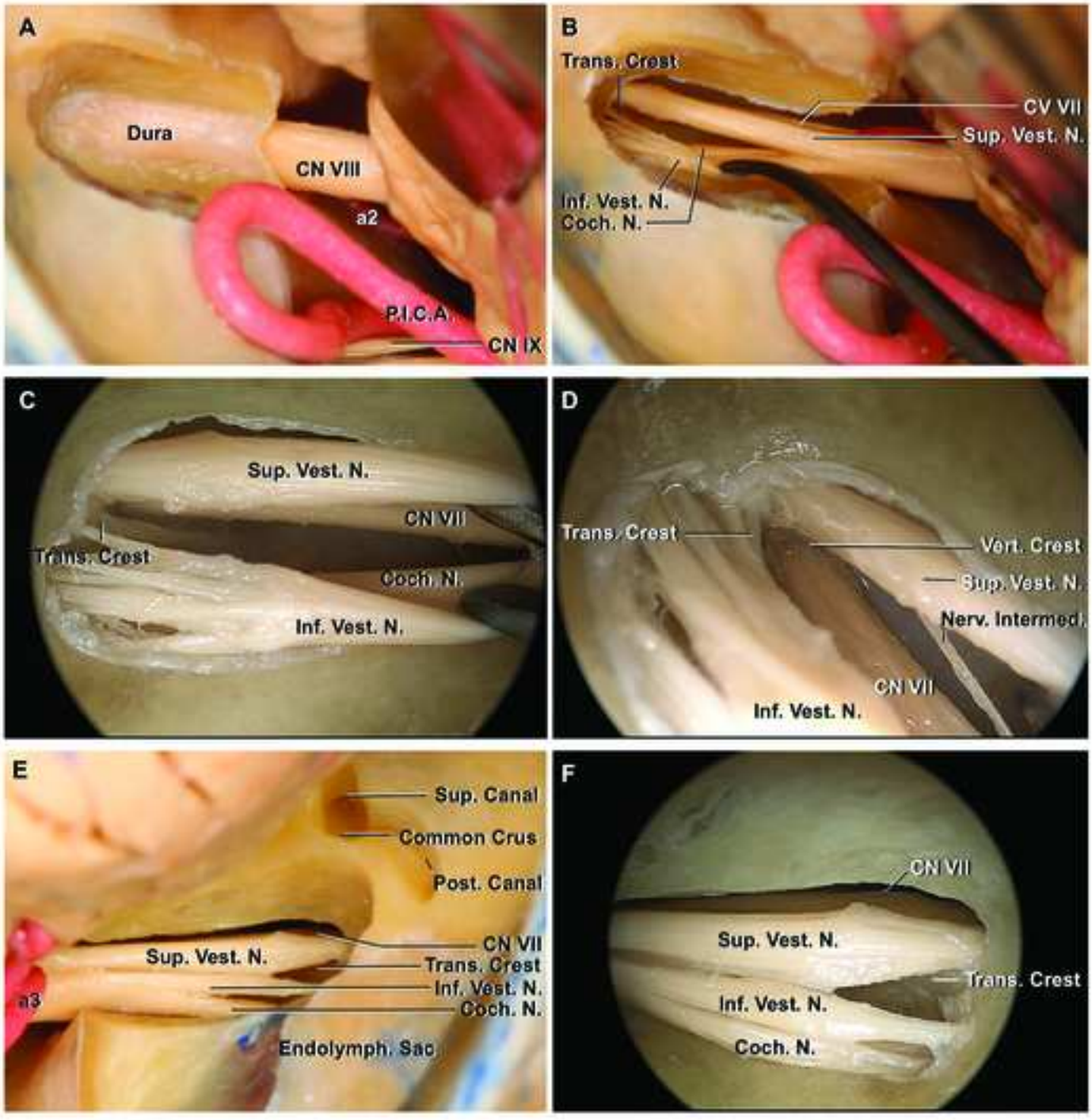

Figure 4A-D

Click here to download high resolution image

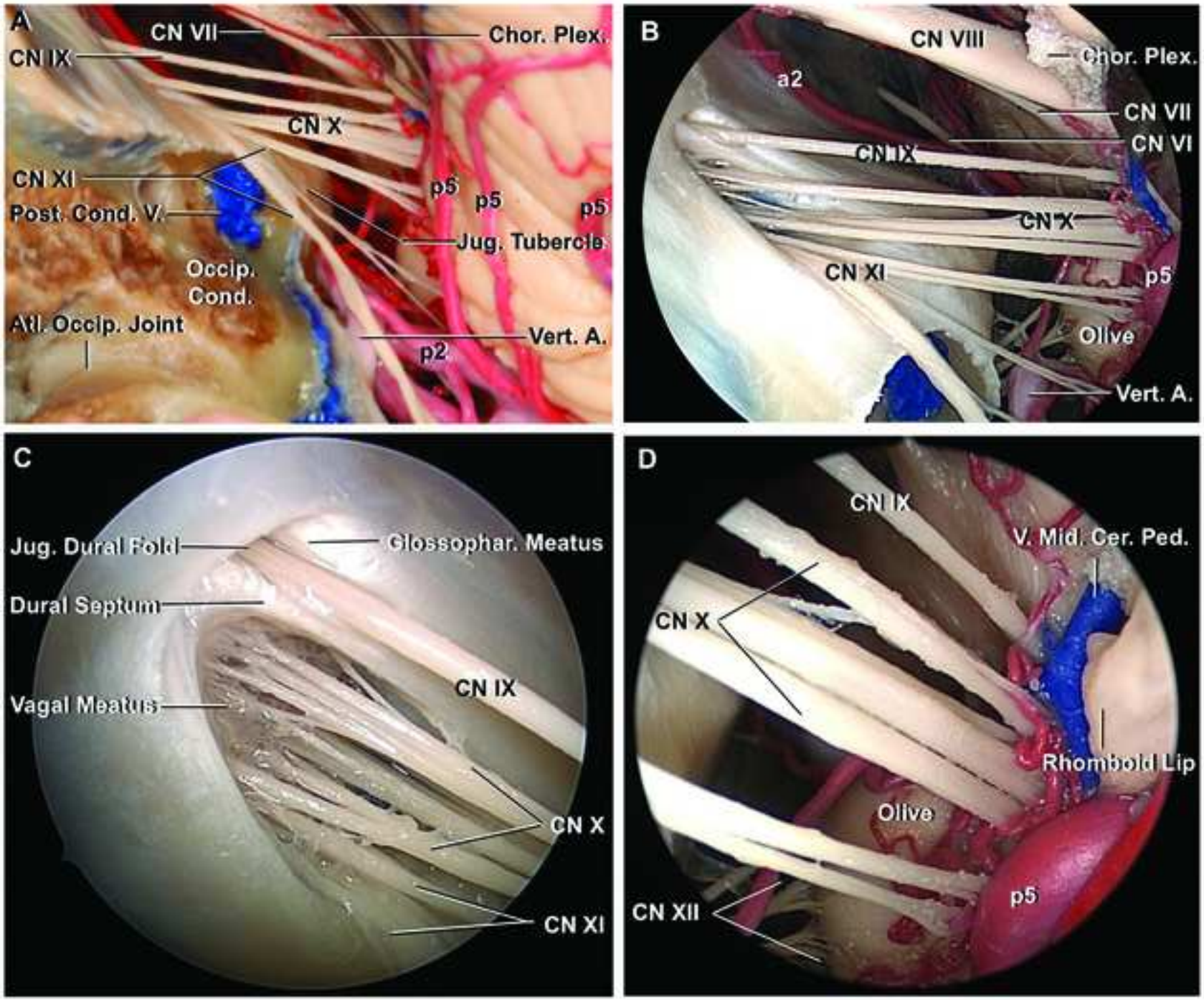

Figure 4E-H

Click here to download high resolution image

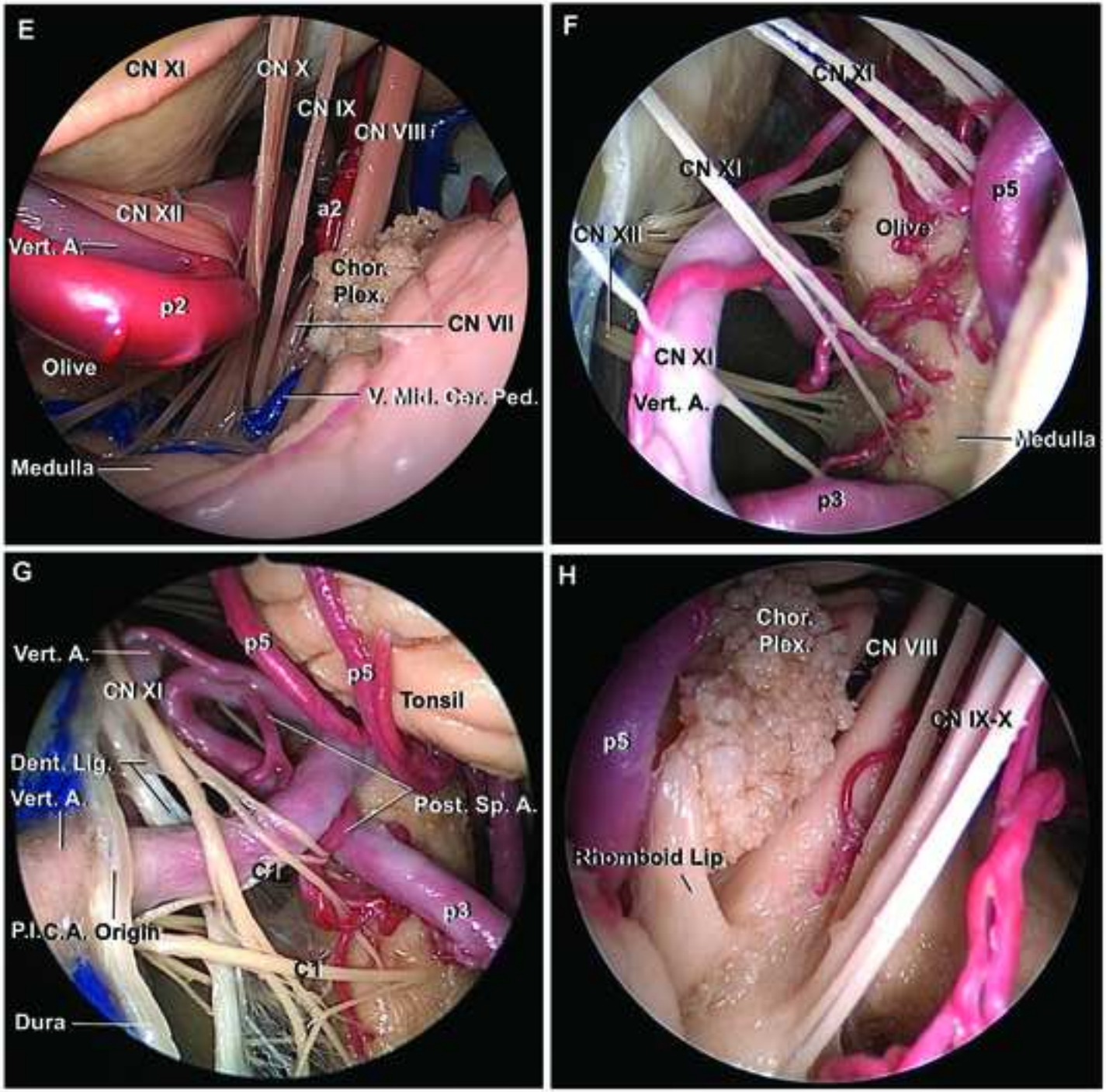

Figure 4I-L

Click here to download high resolution image

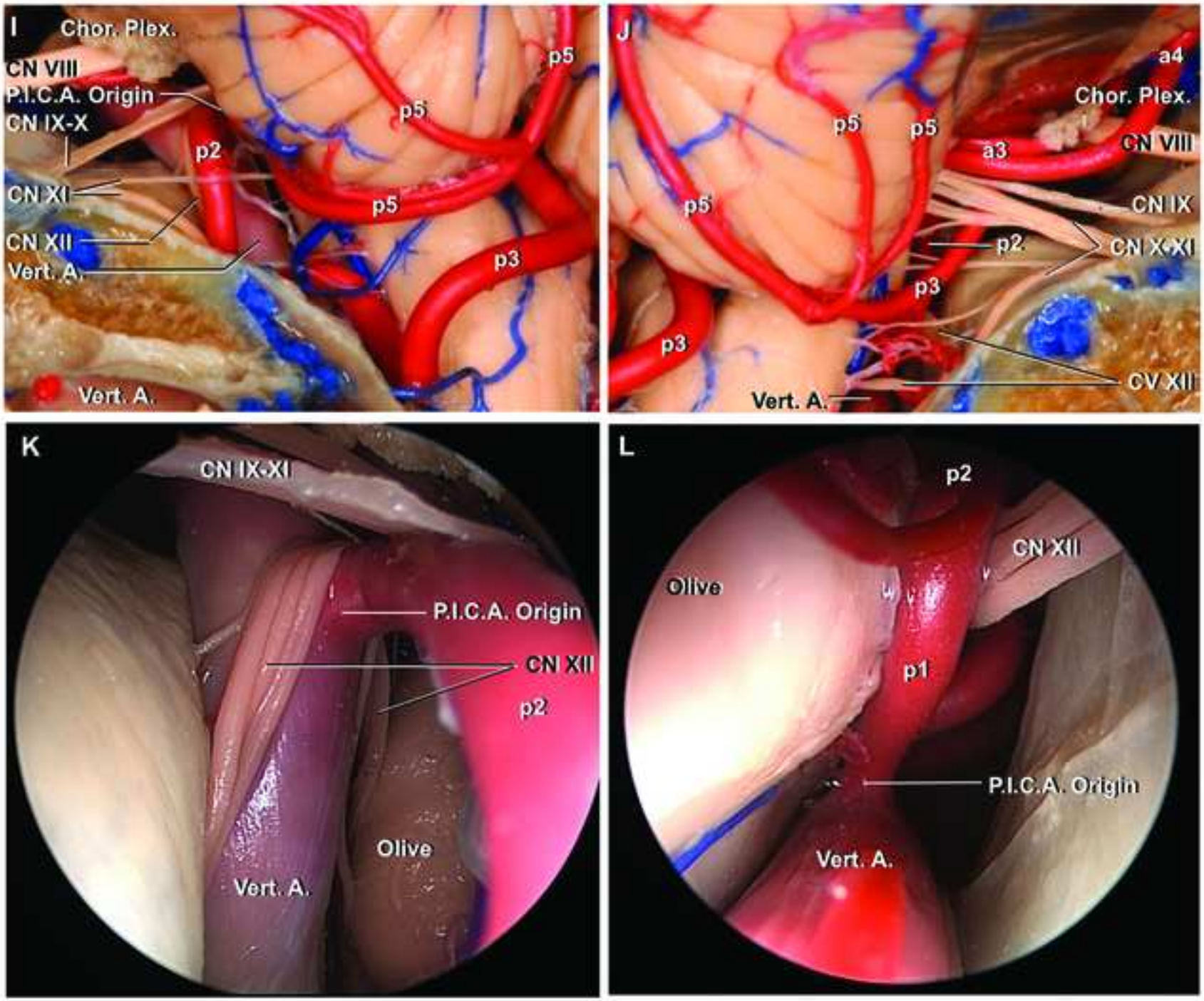

Figure 4M-R

Click here to download high resolution image

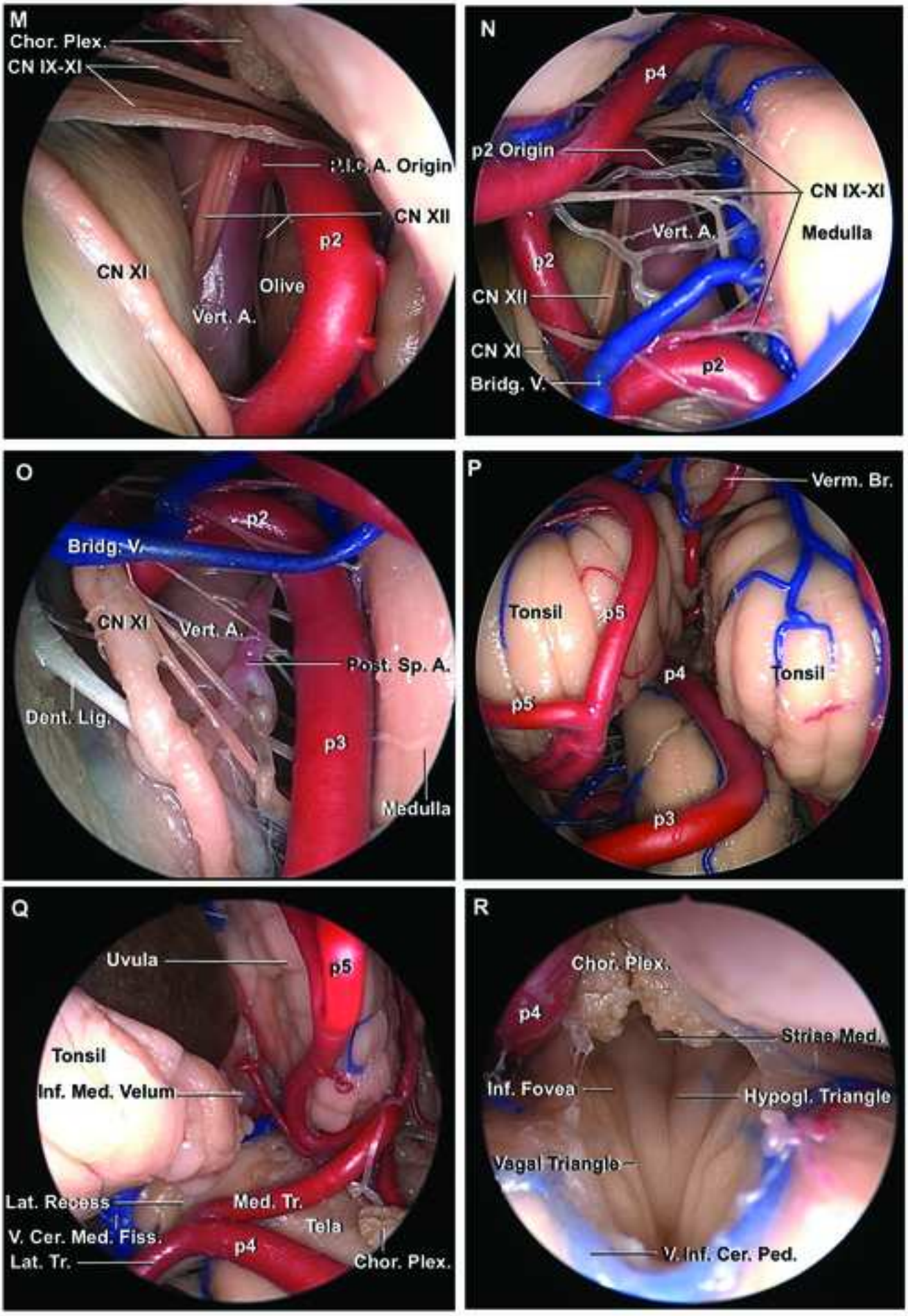

Figure 5A-F

Click here to download high resolution image